

UNIVERSITY MALAYA

ORIGINAL LITERARY WORK DECLARATION

Name of the candidate: **Md. Sohel Rana** (Passport No.:

Registration/Matric No: **KGA 120034**

Name of the Degree: Master of Engineering Science (M. Eng. Sc.)

Title of Project Paper/ Research Report/ Dissertation / Thesis (“this work”):

Tikhonov based well-conditioned asymptotic waveform evaluation technique for heat conduction

Field of Study: Thermal analysis

I do solemnly and sincerely declare that:

- (1) ***I am the sole author /writer of this work;***
- (2) This work is original;
- (3) Any use of any work in which copyright exists was done by way of fair dealings and any expert or extract from, or reference to or reproduction of any copyright work has been disclosed expressly and sufficiently and the title of the Work and its authorship has been acknowledged in this Work;
- (4) I do not have any actual knowledge nor do I ought reasonably to know that the making of this work constitutes an infringement of any copyright work;
- (5) I, hereby assign all and every rights in the copyrights to this Work to the University of Malaya (UM), who henceforth shall be owner of the copyright in this Work and that any reproduction or use in any form or by any means whatsoever is prohibited without the written consent of UM having been first had and obtained actual knowledge;
- (6) I am fully aware that if in the course of making this Work I have infringed any copyright whether internationally or otherwise, I may be subject to legal action or any other action as may be determined by UM.

Candidate’s Signature:

Date:

Subscribed and solemnly declared before,

Witness Signature:

Date:

Name:

Designation:

ABSTRACT

The dual-phase-lag (DPL) heat transfer model is a very stiff partial differential equation which is the mixed derivative of time-space that makes it hard to tackle accurately. For fast transient solution of heat conduction model based on a moment matching technique, researcher generally takes one of two approaches. The first is to linearize the DPL heat conduction equation, where required to introduce extra degree of freedom. The second approach is to work directly using asymptotic waveform evaluation (AWE). But the AWE method is unattractive because the moment matching techniques is intrinsically ill conditioned. In this dissertation, two well-conditioned schemes have developed to reduce the instability of AWE. Furthermore, Fourier heat transfer model and non-Fourier heat transfer model with DPL have analysed by using Tikhonov based well condition asymptotic wave evaluation (TWCAWE) and finite element model (FEM).

The non-Fourier heat conduction has been investigated where the maximum likelihood (ML) and Tikhonov regularization technique has successfully used to predict the accurate and stable temperature responses without the loss of initial high frequency responses. To reduce the increased computational time by Tikhonov based AWE using ML (AWE-ML), another Tikhonov based well-condition scheme called mass effect (AWE-ME) is introduced. AWE-ME showed more stable and accurate temperature spectrum in comparison to asymptotic waveform evaluation (AWE) and also partial Pade AWE without sacrificing the computational time. But the results obtained from AWE-ME scheme are not accurate as AWE-ML.

The TWCAWE method is presented here to study the Fourier and non-Fourier heat conduction problems with various boundary conditions. In this work, a novel TWCAWE method is proposed to overwhelm ill-conditioning of the AWE method for

thermal analysis and also presented for time-reliant problems. The TWCAWE method is capable to evade the instability of AWE and also efficaciously approximates the initial high frequency and delay similar as well-established numerical method, such as Runge-Kutta (R-K). Furthermore, TWCAWE method is found 1.2 times faster than the AWE and also 4 times faster than the traditional R-K method.

ABSTRAK

Dual-fasa-lag (DPL) model pemindahan haba adalah persamaan pembezaan separa sangat sengit yang derivatif campuran masa-ruang yang menjadikannya sukar untuk menangani dengan tepat. Untuk penyelesaian cepat sementara model konduksi haba berdasarkan teknik masa yang hampir sama, penyelidik biasanya mengambil salah satu daripada dua pendekatan. Yang pertama adalah untuk melinearkan persamaan pengaliran haba DPL, di mana perlu untuk memperkenalkan tahap tambahan kebebasan. Pendekatan kedua adalah untuk bekerja secara langsung dengan menggunakan penilaian gelombang asimptot (AWE). Tetapi kaedah AWE itu tidak menarik kerana masa ini yang hampir teknik adalah pada asasnya sakit dingin. Disertasi ini, dua skim yang dingin telah dibangunkan untuk mengurangkan ketidakstabilan AWE. Tambahan pula, Fourier model pemindahan haba dan bukan Fourier pemindahan haba dengan model DPL telah dianalisis dengan menggunakan keadaan baik berdasarkan penilaian Tikhonov gelombang asimptot (TWCAWE) dan model unsur terhingga (FEM).

Bukan Fourier-haba konduksi telah disiasat di mana kebolehjadian maksimum (ML) dan teknik rombakan Tikhonov telah berjaya digunakan untuk meramalkan tindak balas suhu tepat dan stabil tanpa kehilangan balas frekuensi tinggi awal. Untuk mengurangkan masa pengiraan yang meningkat sebanyak Tikhonov AWE berasaskan menggunakan ML (AWE-ML), satu lagi Tikhonov berdasarkan skim yang keadaan yang dipanggil kesan massa (AWE-ME) diperkenalkan. AWE-ME menunjukkan lebih stabil dan tepat spektrum suhu berbanding dengan penilaian asimptot bentuk gelombang (AWE) dan juga sebahagian Pade AWE tanpa mengorbankan masa pengiraan. Tetapi keputusan yang diperolehi daripada skim AWE-ME tidak tepat sebagai AWE-ML.

Kaedah TWCAWE dibentangkan di sini untuk mengkaji Fourier dan bukan Fourier-masalah pengaliran haba dengan pelbagai keadaan sempadan. Dalam karya ini, satu

kaedah TWCAWE novel adalah dicadangkan untuk mengatasi sakit dingin kaedah AWE untuk analisis terma dan turut menyampaikan masalah untuk masa-bergantung. Kaedah TWCAWE mampu untuk mengelakkan ketidakstabilan AWE dan juga efficaciously lebih kurang awal frekuensi tinggi dan kelewatan kaedah berangka yang sama seperti yang mantap, seperti Runge-Kutta (RK). Tambahan pula, kaedah TWCAWE didapati 1.2 kali lebih cepat daripada AWE dan juga 4 kali lebih cepat daripada kaedah RK tradisional.

ACKNOWLEDGEMENTS

In the name of Allah, the most Merciful, the most Beneficent, I would like to take this opportunity to express my utmost gratitude and thanks to the almighty Allah (s.w.t) for giving me such knowledge to do this successful research. My overwhelming thanks go to my honourable supervisors **Dr. Jeevan A/L Kanesan** for their brilliant guidance, support and encouragement to carry out this research work. I am also indebted to my parent, Md. Azizal Haque and Majeda Khatun. Their love, motivation and support always embolden me at every stages of life. It would be impossible to complete this dissertation without their support and encouragement.

Finally, I am also grateful to the University of Malaya, Kuala Lumpur, Malaysia for the financial support under the project ER011-2013A. Last but not the least, I do thank all in the VLSI Lab. for their valuable suggestions, advices and unforgettable helps that really emboldens me throughout the study.

TABLE OF CONTENT

ORIGINAL LITERARY WORK DECLARATION	ii
ABSTRACT	iii
ABSTRAK	v
ACKNOWLEDGEMENTS	vii
TABLE OF FIGURES	xi
LIST OF TABLE.....	xiv
LIST OF SYMBOLS.....	xv
1 CHAPTER 1: INTRODUCTION	1
1.1 Motivation of Research	1
1.2 Problem statement	5
1.3 Objectives	6
2 CHAPTER 2: LITERATURE REVIEW	7
2.1 Introduction	7
2.2 Modes of heat transfer	7
2.3 Analysis of heat transfer problems	8
2.4 Transient heat conduction.....	12
2.5 Heat conduction law	13

2.6	Summary.....	20
3	CHAPTER 3: ANALYTICAL TECHNIQUES FOR HEAT CONDUCTION	23
3.1	Finite element model	23
3.2	Fundamental concept.....	23
3.3	Mathematical formulation for DPL heat conduction model.....	28
3.4	Different analytical technique for dual phase lag heat conduction	29
4	CHAPTER 4: AWE WITH WELL- CONDITIONED STABILITY SCHEME	45
4.1	Tikhonov regularization scheme	45
4.2	AWE with Maximum Likelihood (ML) scheme	46
4.3	T-WCAWE with Mass effect (ME) scheme	47
4.4	Numerical Example	48
5	CHAPTER 5: TICKONOV BASED WCAWE	53
5.1	Motivation	53
5.2	TWCAWE moment matching process	54
5.3	Significance of Z matrix	56
5.4	Breakdown of WCAWE.....	56
5.5	Numerical Example	58

6	CHAPTER 6: SUMMARY AND CONCLUSION	68
6.1	Summary of the finding and conclusion drawn.....	68
7	REFERENCES	71
	PUBLICATIONS.....	76

TABLE OF FIGURES

Figure 1.1: Microprocessor transistors counts against date.....	2
Figure 2.1: Heat transfer through a plane wall	9
Figure 2.2: The three-layer composite slab showing the imposed temperatures on the two sides at the orientation of the coordinate system. The contact between the interfaces is assumed to be thermally perfect, meaning continuity of T	10
Figure 2.3: Schematic of two dimensional heat conduction models	11
Figure 2.4: Schematic of three dimensional heat conduction models	11
Figure 2.5: One-dimensional heat conduction in a solid.....	14
Figure 3.1: Working phase of Finite Element Model.....	24
Figure 3.2: Triangular and rectangular mesh for two dimensional slab.....	25
Figure 3.3: A two dimensional single element.....	29
Figure 3.4: Flow of AWE algorithms.....	40
Figure 3.5: Dimensionless temperature distribution along the top edge of slab at $Z_b = 0.0001$	41
Figure 3.6: Dimensionless temperature distribution along the top edge of slab at $Z_T = 0.0001$ after applying partial Pade' approximation	42
Figure 3.7: Comparison between AWE (after applying partial Pade' approximation) and Runge–Kutta for case $Z_b = 0.0001$	44
Figure 4.1: Normalized temperature response spectrum along centre of the slab in the case of $Z_b = 0.5$	48

Figure 4.2: Normalized temperature response spectrum along centre of the slab in the case of $Z_b=0.05$	49
Figure 4.3: Normalized temperature response spectrum along centre of the slab for the case of $Z_b=0.0001$	49
Figure 4.4: Comparison with T-WCAWE with ML, T-WCAWE with ME, Runge-Kutta and AWE using partial Pade in the case of $Z_b=0.05$	50
Figure 4.5: Comparison of T-WCAWE with ML, T-WCAWE with ME, Runge-Kutta and AWE with partial Pade for the case of $Z_b=0.0001$	50
Figure 4.6: Comparison of AWE-ML (with Tikhonov), AWE-ML (without Tikhonov) and ICAWE (without Tikhonov) for $Z_b=0.0001$	51
Figure 5.1: Instantaneous heat impulse	59
Figure 5.2: Constant heat imposed	59
Figure 5.3: Periodic heat imposed	59
Figure 5.4: Two-dimensional slab subjected to instantaneous temperature rise on left edge.....	60
Figure 5.5: Normalized temperature responses for Fourier heat conduction	61
Figure 5.6: Fourier temperature responses along the centre of the slab for different time	61
Figure 5.7: Normalized temperature responses along the Centre of the slab for $Z_b=0.5$, 0.05 and for $Z_b=0.0001$ with instantaneous heat imposed, A) at node 5, B) at node 59	63
Figure 5.8: Normalized temperature distribution along centre of the slab for $Z_b=0.5$, 0.05 and $Z_b=0.0001$ with instantaneous heat imposed (A) at time 0.005 (B) at time 0.05 (C) at time 0.1 (B) at time 0.5	64

Figure 5.9: Normalized temperature response along centre of the slab for $Z_b=0.5$, 0.05 and $Z_b=0.0001$ with periodic heat executed, A) at node 5, B) at node 59.....65

Figure 5.10: Normalized temperature distribution along the centre of the slab for three values of Z_b with periodic heat levied, A) at time 0.005, B) at time 0.05, C)at time 0.1, D) at time 0.565

Figure 5.11: Normalized Temperature response along for three values of Z_b with constant heat imposed, A) at node 5, B)at node 5966

Figure 5.12: Normalized temperature dissemination along the centre of the slab for three values of Z_b with constant heat imposed, A) at time 0.005, B) at time 0.05, C)at time 0.1, D) at time 0.566

LIST OF TABLE

Table 3.1: Fourth order Runge-Kutta method	30
Table 5.1: ALGORITHM 1	55
Table 5.2: ALGORITHM 2	57
Table 6.1: Simulation time required by different method.	69

LIST OF SYMBOLS

Symbols	Description
A	Area of element
K_c	Thermal conductivity
L	Length of element
K_x	Thermal conductivities in the x direction
K_y	Thermal conductivities in the y direction
C	Volumetric heat capacity
h	Thickness
q	Thermal flux
κ_b	Phase delay of longitudinal temperature gradient in regard to local temperature
κ_a	Phase delay of heat flux in regard to local temperature
ρ	is material density
T	Temperature
t	time
β	standardized time
Z_b	standardized phase delay for temperature gradient
Z_a	standardized phase delay for heat flux
σ	Thermal diffusivity.
K	Conductivity matrix
f	Load vector
[a]	Nodal moments
p	Poles
r	rasidue
K(s)	compound matrix
F(s)	compound excitation vector
f	Frequency
I	Identity matrix
h_c	regulation parameter
K	grid aspect ratio
D_c	Consistent matrices
D_L	row sum-lumped mass matrices
τ	relaxation time
ε	Normalized distance in X direction

ψ	Normalized distance in Y direction
q	Number of Pade
M_n	Moments
f_0	Initial frequency

1 CHAPTER 1: INTRODUCTION

1.1 Motivation of Research

The unprecedented success of information technology has focused by semiconductor industry to advance at dramatic rate. The increasing demand for higher performance in integrated circuits (ICs) results in faster switching speed, greater number of transistors , increased functional density and large chip size. Subsequently, the communication, supported by on chip interconnects, between devices and circuits blocks is becoming multifaceted and challenging problems. The connection of miniaturized and closely packed transistors required reduced wire cross-section in local levels. As device sizes continue to shrink and integration densities continue to upsurge, interconnect delays have become precarious bottlenecks of chip performances.

Moore's law is based on observation, that is; over the history of computing hardware, the number of transistors on integrated circuits doubles approximately in every two years. This forecast has proven to be accurate, in part because the law is now used in the semiconductor industry to guide long-term planning and to set targets for development. The competences of many digital electronic devices are sturdily linked to Moore's law: processing speed, memory capacity, sensors and even the number and size of pixels in digital cameras. All of these are improving at roughly exponential rates as well. This exponential improvement has dramatically enhanced the impact of digital electronics in nearly all sector of the global economy. Moore's law describes a driving force of technological and social change in the late 20th and early 21st centuries.

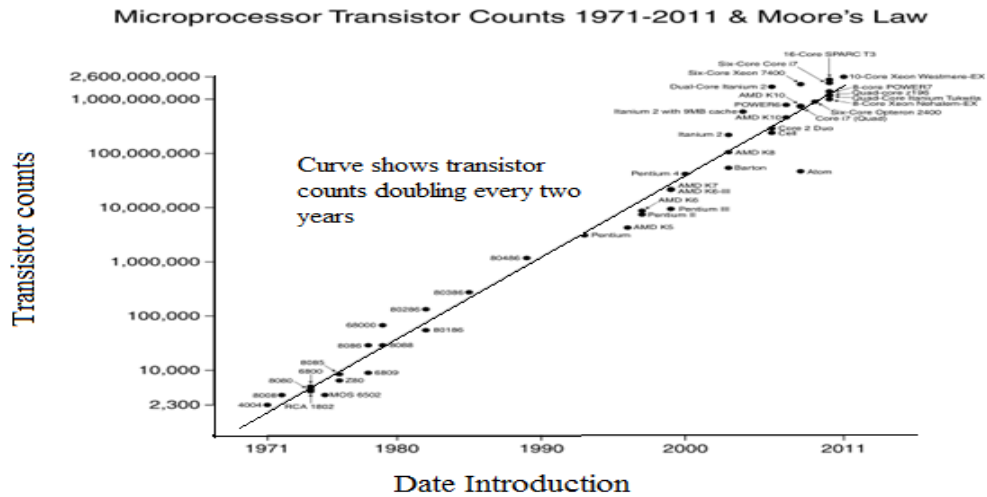


Figure 1.1: Microprocessor transistors counts against date

The increasing demand for additional multifaceted VLSI circuits with higher performance is leading to higher power dissipation and enlarged the thermal problems. Thermal issues are hastily becoming one of the most challenging problems in high-performance chip design due to ever-increasing device count and clock speed(Gwennap, 1998). Thermal management is vital to the growth of upcoming generations of microprocessors, integrated network processors, and systems-on-a chip. At the circuit level, temperature variations in the substrate and interconnect lines have important implications for circuit performance and reliability(Banerjee, Mehrotra, Sangiovanni-Vincentelli, & Hu, 1999; Rzepka, Banerjee, Meusel, & Hu, 1998).

Designing a cost viable power electronics system requires careful consideration of the thermal domain as well as the electrical domain. Over designing the system enhances needless cost and weight; under designing the system may lead to overheating and even system failure.

Finding an optimized solution requires a good understanding of how to predict the operating temperatures of the system's power components and how the heat generated by those components affects adjacent devices. No single thermal analysis tools or

technique works best in all conditions. Good thermal valuations require for making a grouping of analytical calculations using thermal stipulations, empirical analysis and thermal modelling.

Thermal management are becoming prevail thoughts because more and more composite difficulties are causing by the fast progress in semiconductor devices and their packaging. The electrical performance of these devices and its reliability are strongly temperature dependent. It is believable that, to investigate and avert thermal failure of ICs chip, two operation criteria have to be considered: the average junction temperature of the chip and the difference of temperature among the components (Suhir & Lee, 1988).

The purpose of thermal control in the package design is to keep the junction temperatures of all components below a maximum tolerable level. There is a approximately exponential dependence of failure rate on components temperature which depends on packaging method and the heat dissipation of chip. This kind of failure is constantly related with mechanical fracture as well as loss of electrical functions. Another kind of failure arising from temperature difference among the components related to critical electrical paths. The sensitivity of a component performance to its temperature difference becomes an important concern for a high-speed system because of the problem of signal skew. As a result, the junction temperatures of various components should be kept within a specified range for a high performance system.

A large amount of research is focused on the thermal analysis of IC chips and its packaging on the background of thermal reliability. In the analysis of heat transport of IC chip Fourier's heat conduction equation based on diffusion mechanism was frequently used. It is known that, this equation suggests a presumption of infinite thermal propagation speed. The Fourier forecast may underestimate the peak

temperature during a fast transient process. The applications of non-Fourier heat conduction equation formerly proposed by Maxwell (Maxwell, 1867) and then revised by other researchers (Vernotte, 1958). Its earlier successful application was to forecast the rapid transient heat conduction process in chemical and the process engineering also in the process of laser pulse heating (Gibbons, Sigmon, & Hess, 1981). In microelectronic engineering, hyperbolic heat conduction model was used in thermal analysis of semiconductor processing or laser annealing (Bloembergen, Kurz, Liu, & Yen, 1981). Recently Bai et al (Bai & Lavine, 1991) carried out a detailed investigation on the heat transport in superconducting electronic devices based on hyperbolic heat conduction equation.

The most vital feature of IC chips is its high frequency electrical pulse. A pervasive theme in the microelectronic industry has been miniaturization and increasing function density. Circuit density continues to upsurge at a rate of about 30% per year which is accompanied largely reducing in feature size of the circuit elements. This continuous shrinkage in feature size also leads the operating speed to a very high level and the cycle time can be as short as a few nanoseconds. The duration of the corresponding heat pulse can be as short as 100 picoseconds. Consequently, the IC elements would undergo a very rapid transient process, which is the main basis of taking the non-Fourier conduction effects in IC chip. So, an analysis of non-Fourier heat conduction in IC chip is become getting importance in present years. The main concerns of present-day research are faster and accurate temperature prediction of non-Fourier heat conduction model in IC chip.

A number of traditional iterative solvers can be found to analyse the Fourier and non-Fourier heat conduction model. In numerical analysis, the Runge–Kutta (RK) method is an important family of implicit and explicit iterative methods, which are used

in temporal discretization for the approximation of solutions of ordinary differential equations. The results accuracy of RK method is sturdily depends on choice of step size. Small step size provides good results; but takes additional simulation time. In case of heat transfer problem, Runge-Kutta (RK) method is very well known and the results obtained from RK are taken as benchmark in comparison(Loh, Azid, Seetharamu, & Quadir, 2007)This iterative method is undeniably very precise, but computationally expensive.

To reduce the computational time, in past few years; fast transient heat transfer model has been analysed by using moment matching based technique known as Asymptotic Waveform Evaluation (AWE) method (Loh et al., 2007). The AWE method is much faster solver compare to any traditional iterative solver. Taylor's series has been used to expand the AWE transfer function. Then the required moments are found from the coefficient of Taylor's series. AWE technique is able to solve up to three-dimensional models (Sun & Wichman, 2004). The limitation of AWE model is, the model cannot forecast the temperature responses accurately as it is ill-conditioned moment matching. Then Loh et al. (Loh et al., 2007) developed a scheme called partial Pade AWE, which is also based on the AWE to reduce the instability of AWE,. In partial Pade AWE, arbitrarily selected poles and residues from any heat imposed boundary has taken to calculate the temperature responses of the whole system. As results, the technique is also unable to predict the actual temperature responses.

1.2 Problem statement

Controversy statements, limitation of available methods to analyze the thermal problems are deemed barrier in heat conduction. This study intends to analyze the Fourier and Non-Fourier heat conduction equation in diverse boundary condition. Specifically, the study seeks the following questions,

- ❖ What is the limitation of previous analytical methods?
- ❖ How we can overcome these limitations and which method is best for transient heat conduction?
- ❖ Does propose method is accurate?

1.3 Objectives

To solve the above mentioned problems, the objectives of this study are considered as follows:

- ❖ Study about Finite element model (FEM), Fourier & Non-Fourier heat conduction equation. Design FEM for Non-Fourier heat conduction analysis in ICs floor planning.
- ❖ Simulate Runge-Kutta (RK) and Asymptotic Waveform Evaluation (AWE) for Non-Fourier heat conduction equation.
- ❖ Develop a new algorithm and compare the results with previous techniques to see the improvement.
- ❖ To verify the accuracy of proposed algorithm in various boundaries conditions.

2 CHAPTER 2: LITERATURE REVIEW

2.1 Introduction

Heat transfer describes the exchange of thermal energy between physical systems depending on the temperature and pressure, by dissipating heat. Systems which are not isolated may decrease in entropy. Most objects emit infrared thermal radiation near room temperature. Heat transfer generally takes place by three modes such as conduction, convection and radiation. Heat conduction, in mainstream of real states, occurs as a result of combinations of these modes of heat transfer. The modes of heat transfer has discussed in following section.

2.2 Modes of heat transfer

Conduction is the transfer of thermal energy between neighbouring molecules in a substance due to a temperature gradient. It always takes place from a region of higher temperature to a region of lower temperature, and acts to balance the temperature differences. Conduction needs matter and does not involve any bulk motion of matter. Conduction takes place in all forms of matter such as solids, liquids, gases and plasmas. In solids, it is due to the combination of vibrations of the molecules in a lattice and the energy transport by free electrons. In gases and liquids, conduction is due to the collisions and diffusion of the molecules during their random motion.

Convection occurs when a system becomes unstable and begins to mix by the movement of mass. A common observation of convection is of thermal convection in a pot of boiling water, in which the hot and less-dense water on the bottommost layer moves upwards in plumes, and the cool and denser water near the topmost of the pot likewise sinks. Convection more likely occurs with a greater variation in density between the two

fluids, a larger acceleration due to gravity that drives the convection through the convecting medium.

Radiation describes any process in which energy emitted by one body travels through a medium or through space absorbed by another body. Radiation occurs in nuclear weapons, nuclear reactors, radioactive radio waves, infrared light, visible light, ultraviolet light, and X-rays substances.

2.3 Analysis of heat transfer problems

The key of the heat conduction problems contains the functional dependence of temperature on various parameters such as space and time. Obtaining a solution means determining a temperature distribution which is reliable with conditions on the boundaries. In general, the flow of heat takes place in diverse spatial coordinates. In some cases, the analysis is done by considering the variation of temperature in one-dimension (1D), two-dimension (2D) and three-dimension (3D). In the most common case, heat transfer through a medium is three-dimensional. However, some problems can be classified as two- or one dimensional depending on the relative magnitudes of heat transfer rates in diverse ways and the level of precision that is preferred.

2.3.1 One dimensional heat conduction

The term "one dimensional" refers to the fact that only one coordinate is required to define the spatial variation of the dependent variables. Hence, in a one-dimensional system, temperature gradients exist along a single coordinate direction, and heat transfer occurs completely in that direction. The system is characterized by steady state conditions if the temperature at each point is independent of time.

In the case of one dimensional heat conduction in a plane wall, temperature is a function of the x coordinate only and heat is transferred completely in that direction. In

Figure 2.1, a plane wall splits two fluids of unlike temperatures. Heat transfer occurs by conduction from the upper temperature side at T_1 to one surface of the wall at T_2 by conduction through the convection from the other surface of the wall at to the lower temperature side. We begin by considering conditions within the wall. We first determine the temperature distribution, from which we can then obtain the conduction heat transfer rate. For one dimensional, steady state conduction in a plane wall with no heat generation and constant thermal conductivity, the temperature varies linearly with x . Now, we have temperature distribution, we may use Fourier's law, to determine the conduction heat transfer rate. That is,

$$q_x = -K_c A \frac{dT}{dx} = \frac{K_c A}{L} (T_1 - T_2) \quad (2.1)$$

Where, A is the area of the wall normal to the direction of heat transfer and for the plane wall; it is a constant and independent of x . The heat flux is

$$q_x = \frac{Q}{A} = \frac{K_c}{A} (T_1 - T_2) \quad (2.2)$$

The broad solution for the temperature distribution is first obtained by solving the suitable form of the heat equation. The boundary conditions are then applied to obtain the particular solution, which is used with Fourier's law to determine the heat transfer rate. Note that we have chosen to describe the surface temperatures at $x=0$ and $x=L$ as boundary conditions.

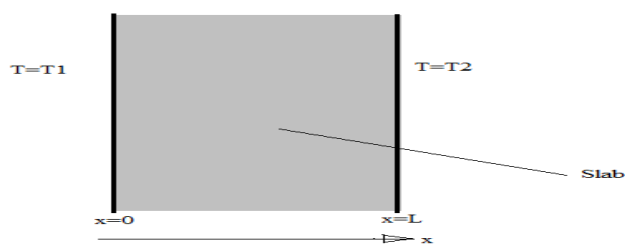


Figure 2.1: Heat transfer through a plane wall

One dimensional analysis helps to model the system in one layer, two layer and three layer systems that define several boundary conditions. Based on the symmetries observation in the two and three-layer problems, can be framed a conjectured n layer solution for the one-dimension multi-layer slab(Sun & Wichman, 2004). Consider a composite slab consisting of three parallel layers as shown in Figure 2.2. Let K_1 , K_2 , and K_3 be the thermal conductivities, α_1 , α_2 , and α_3 be the thermal diffusivities and d_1 , d_2 , and d_3 be the thickness of the first, second and third layers, respectively.

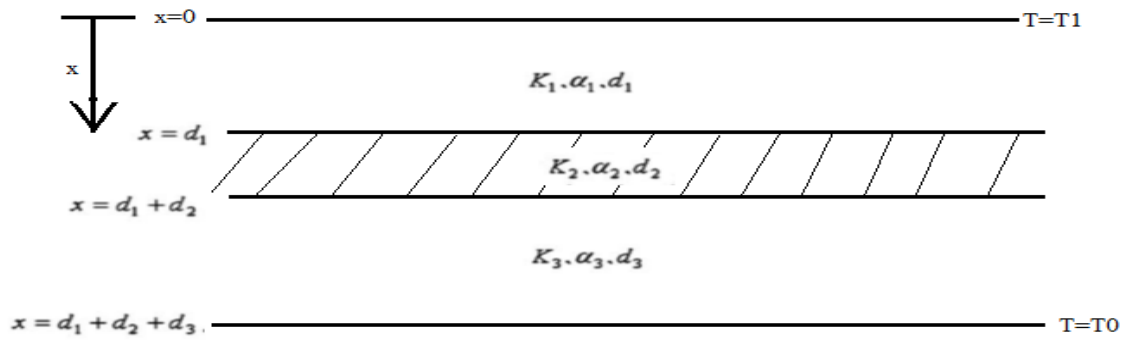


Figure 2.2: The three-layer composite slab showing the imposed temperatures on the two sides at the orientation of the coordinate system. The contact between the interfaces is assumed to be thermally perfect, meaning continuity of T .

2.3.2 Two dimensional heat conduction

In the case of two dimensions, for the temperature $T(x, y, t)$; the governing partial differential heat conduction equation is,

$$\left(\frac{\partial}{\partial x} \left(K_x \frac{\partial T}{\partial x} \right) + \frac{\partial}{\partial y} \left(K_y \frac{\partial T}{\partial y} \right) \right) + Q = C \frac{\partial T}{\partial t} \quad (2.3)$$

The thermal conductivities in the x , y -directions have denoted by, K_x and, K_y , (W/(m.K)), respectively. The volumetric heat capacity is denoted by C , (J/(m³K)), which is equivalent to the density times the specific heat capacity ($C = \rho.C_p$). The thermal conductivities in the two directions are usually the same ($K_x=K_y$). The internal heat

generation is often considered as zero. In the steady-state case, the right-hand side of Equation (2.3) is zero.

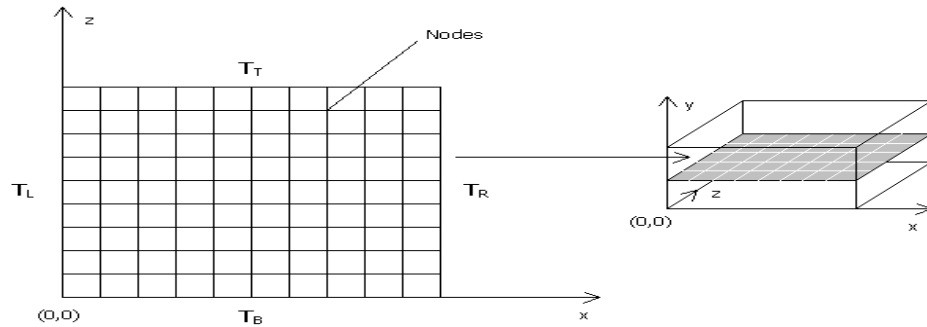


Figure 2.3: Schematic of two dimensional heat conduction models

2.3.3 Three dimensional heat conduction

In the case of two dimensions, for the temperature $T(x, y, t)$; the governing partial differential heat conduction equation is,

$$\left(\frac{\partial}{\partial x} \left(K_x \frac{\partial T}{\partial x} \right) + \frac{\partial}{\partial y} \left(K_y \frac{\partial T}{\partial y} \right) + \frac{\partial}{\partial z} \left(K_z \frac{\partial T}{\partial z} \right) \right) + Q = C \frac{\partial T}{\partial t} \quad (2.4)$$

The thermal conductivities in the x , y and z -directions are denoted by, K_x , K_y , and K_z (W/(m.K)), respectively. The volumetric heat capacity is denoted by C , (J/(m³K)), which is equivalent to the density times the specific heat capacity ($C = \rho.C_p$). The thermal conductivities in three directions are usually considered as ($K_x=K_y=K_z$). The internal heat generation is also considered as zero. In the steady-state case, the right-hand side of Equation (2.4) is zero.

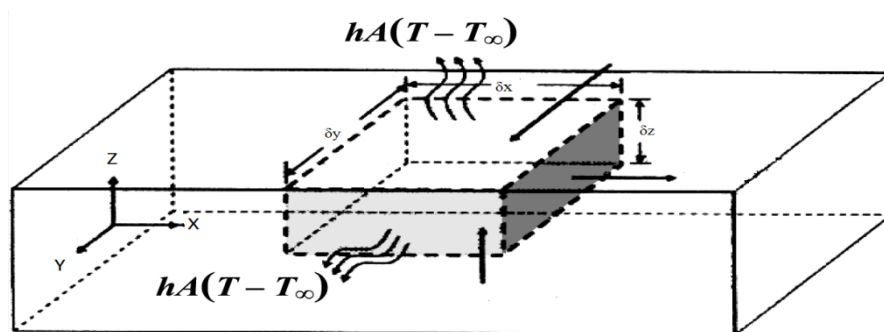


Figure 2.4: Schematic of three dimensional heat conduction models

2.4 Transient heat conduction

2.4.1 Steady state heat conduction analysis

A steady-state thermal analysis forecasts the effects of steady thermal loads on a system. A system is said to be reached steady state when the variation of several parameters namely, temperature, pressure and density are changing with time but the temperature responses are saturated. A steady-state analysis also can be considered as the last step of a transient thermal analysis. We can use steady-state thermal analysis to determine the temperatures, heat flow rates, thermal gradients and heat fluxes in an object which do not vary over time. A steady-state thermal analysis may be either linear, by assuming constant material properties or can be nonlinear case, with material properties varying with temperature. The thermal properties of most material do vary with temperature, so the analysis becomes nonlinear. Furthermore, by considering radiation effects system also become nonlinear.

2.4.2 Unsteady state heat conduction analysis

Before a steady state condition has reached, a certain amount of time has passed after the heat transfer process is initiated to allow the transient conditions to be disappearing. For example, while determining the rate of heat flow through wall, we do not consider the period during which the furnace starts up and the temperature of the interior, as well as those of the walls, steadily increase. We frequently assume that, this period of transition has passed and that steady-state condition has been established. In the temperature distribution in an electrically heated wire, we usually neglect warming up period. Yet we know that, when we turn on a toaster, it takes some time before the resistance wires attain maximum temperature, although heat generation starts

instantaneously when the current begins to flow. Another type of unsteady-heat-flow problem involves with periodic variations of temperature and heat flow.

Periodic heat flow occurs in internal-combustion engines, air-conditioning, instrumentation, and process control. For example the temperature inside stone buildings remains quite higher for several hours after sunset. In the morning, even though the atmosphere has already become warm, the air inside the buildings will remain comfortably cool for several hours. The reason for this phenomenon is the existence of a time lag before temperature equilibrium between the inside of the building and the outdoor temperature.

Another typical example is the periodic heat flow through the walls of engines where temperature increases only during a portion of their cycle of operation. When the engine warms up and operates in the steady state, the temperature at any point in the wall undergoes cycle variation with time. While the engine is warming up, a transient heat-flow phenomenon is considered on the cyclic variations.

2.5 Heat conduction law

2.5.1 Fourier heat conduction

The mathematical theory of heat conduction was developed early in the nineteenth century by Joseph Fourier. The theory was based on the results of experiments similar to that illustrated in Figure 2.5, in which one side of a rectangular solid is held at temperature T_1 , while the opposite side is held at a lower temperature, T_2 . The other four sides are insulated so that, heat can flow towards in x -direction only. For a given material, it is found that; the heat flow rate, q_x , at which heat (thermal energy) is moved from the hot side to the cold side is proportional to the cross-sectional area A , across which the heat flows and the temperature difference, $T_1 - T_2$; and also inversely

proportional to the thickness, B , of the material. The mathematical formulation can be symbolized as follows:

$$q_x \propto \frac{A(T_1 - T_2)}{B}$$

Writing this relationship as equality, we have:

$$q_x = \frac{K_c A (T_1 - T_2)}{B} \quad (2.5)$$

K_c is thermal conductivity.

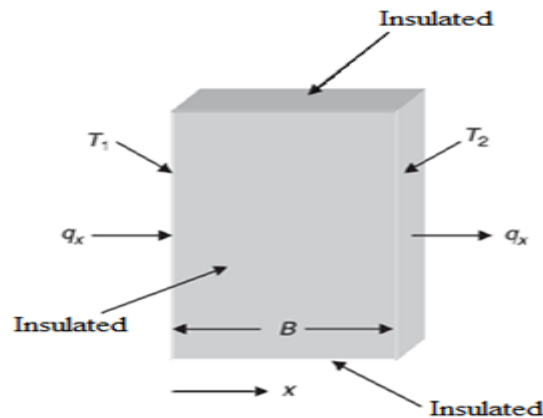


Figure 2.5: One-dimensional heat conduction in a solid

The form of Fourier's law given by Equation (2.5) is effective only when the thermal conductivity can be assumed constant. A more common result can be obtained by writing the equation for an element of differential thickness. Thus, let the thickness be Δx and let

$\Delta T = T_2 - T_1$. Substituting in Equation (2.5) gives

$$q_x = -\frac{K_c A \Delta T}{\Delta x}$$

Now in the limit as Δx approaches zero,

$$\frac{\Delta T}{\Delta x} \rightarrow \frac{dT}{dx}$$

$$q_x = -K_c A \frac{dT}{dx} \quad (2.6)$$

Now, the Fourier heat conduction equation denoted by (2.6) is not subject to the limit of constant K_c . Hence, Equation (2.6) is the general one-dimensional form of Fourier's law. The negative sign is necessary because heat flows in the positive x -direction when the temperature decreases in the x -direction. Thus, according to the standard sign convention that q_x is positive when the heat flow is in the positive x -direction, q_x must be positive when dT/dx is negative.

2.5.1.1 Fourier's laws inconsistency

Consider for example, a flat slab and apply at a given instant; a supply of heat to one of its faces. Then according to Fourier law ($q = -K_c \nabla \theta$) there is an instantaneous effect at the other face. Loosely speaking, according to Fourier law and also due to the intrinsic parabolic nature of the partial differential equation, the diffusion of heat gives rise to infinite speeds of heat propagation. This conclusion, named by some authors the paradox of instantaneous heat propagation, is not physically realistic because it clearly violates one important principle of the Einstein's special theory of relativity. The above mentioned contradictions between the Fourier's heat conduction laws and the theory of relativity can be overcome using several models. Furthermore, Fourier heat conduction law unable to explain some special case of heat transfer such as temperature near absolute zero, extreme thermal gradients, high heat flux conduction, short time behavior. To avoid these limitations, researcher has developed phase lag based heat conduction model that able to account the relaxation time.

2.5.2 Non Fourier heat conduction

2.5.2.1 The generalized lagging response, formulation of the model: The Cattaneo-vernotte (CV) model

The CV model familiarizes the thought of the relaxation time, τ , as the build-up time for the start of the thermal flux after a temperature gradient is rapidly executed on the

sample. Suppose that, as a consequence of the temperature existing at each time instant, t , the heat flux seems only in a subsequent instant, $t + \tau$. Under these conditions Fourier's Law adopts the form as following equation (2.7)

$$q(x, t + \tau) = -k_c \frac{\partial T(x, t)}{\partial x} \quad (2.7)$$

If τ is small (as it should be, because otherwise the first Fourier's law would fail when explaining every day phenomena), then we can expand the heat flux in a Taylor Series around $\tau = 0$ obtaining

$$q(x, t + \tau) = q(x, t) + \tau \frac{\partial T(x, t)}{\partial x} \quad (2.8)$$

Substituting Equation (2.8) in Equation (2.7) leads to the revised Fourier's law of heat conduction or CV equation that states

$$\tau \frac{\partial \vec{q}}{\partial t} + \vec{q} = -k \vec{\nabla} T \quad (2.9)$$

Here, the time derivative term makes the heat propagation speed finite. Equation (2.9) tells us that, the heat flux does not appear instantaneously but it grows gradually with a build-up time, τ . For macroscopic solids at ambient temperature this time is of the order of 10^{-11} s, so that for practical purposes the use of Fourier is adequate, as daily experience shows.

$$\nabla^2 T - \frac{1}{\alpha} \frac{\partial T}{\partial t} - \frac{1}{u^2} \frac{\partial^2 T}{\partial t^2} = -\frac{1}{k_c} \left(\mathcal{Q} + \tau \frac{\partial \mathcal{Q}}{\partial t} \right) \quad (2.10)$$

2.5.2.2 Fields of application

The CV model although necessary has some disadvantages among them:

- i) The hyperbolic differential Equation (2.10) is complicated from the mathematical point of view and in the majority of the physical situations has non analytical solutions.
- ii) The relaxation time of a given system is in general an unknown variable. Therefore care must be taken in the interpretation of its results. Nevertheless, several examples can be found in the literature.

Due to these early works the speed u is often called the second sound velocity. More recently Tzou reported on phenomena such as thermal wave resonance (Yu Tzou, 1991) and thermal shock waves generated by a moving heat source (Ozisik & Tzou, 1994). Very rapid heating processes must be described by using the CV model too, such as those taking place during the absorption of energy coming from ultra-short laser pulses (Marín, Marin, & Hechavarría, 2005) and during the gravitational collapse of some stars (Govinder & Govender, 2001), as many numerical and analytical calculations indicate.

On the other hand, one actual field of rapid development is nano-science and nanotechnology, in which several studies have reported nano-scale heat transfer behaviour deviating significantly from that at the normal scale (X.-Q. Wang & Mujumdar, 2007). It is well known that, thermal time constants, τ_c , characterizing heat transfer rates depends strongly on particle size and on its thermal diffusivity, α . One can assume that, for spherical particles of radius L , these times scale proportional to L^2/α . As for condensed matter, the order of magnitude of α is 10^{-6} m²/s for spherical particles having nanometric diameters, says for example between 100 and 1 nm, we obtain for these times values ranging from about 10 ns to 1ps, which are very close to the above mentioned relaxation times.

At these short time scales, Fourier's laws unable to work in their initial forms. In this field and for continuous transient heating the work of Vadasz *et al.* (Vadasz, Govender, & Vadasz, 2005) is illustrative. On the basis of theoretical calculations and experimental

data these authors demonstrated that, the hyperbolic heat transfer could have been the cause of the extraordinary heat transfer enhancement revealed experimentally in colloidal suspensions of nanoparticles, the so-called nanofluids. The calculated results show that, the apparent thermal conductivity obtained via Fourier based relationships could indeed produce results showing substantial enhancement of the effective thermal conductivity calculated by means of the CV hyperbolic model. However, as the values of the times τ and τ_c are in general not well known, the interpretation of experimental data is problematic. On the other hand the authors show the results of numerical solutions for the significant case of a sample experiencing a sudden temperature change at the surface by heating using a pulsed laser beam. Finally, for a particular case of periodical modulated sample heating (Marín, Marín-Antuña, & Díaz-Arencibia, 2002), demonstrated the very important result that for low modulation frequencies, when compared with $1/\tau$, the CV model leads to the conventional Fourier's formalism. Inspired to a certain extent in the above mentioned that, it has been recently suggested the possibility to incorporate the so-called photo thermal (PT) techniques (Marín, 2013), that use periodical heating to generate the measured signals, to the vast arsenal of methods used for thermal characterization, with the great advantage among these that the results of PT experiments can be interpreted using much simpler Fourier's laws based models.

2.5.3 Two phase lag heat conduction model

The non-Fourier heat transfer induces thermal waves by delaying the response between heat flux and temperature gradient. This delay may represent time needed to accumulate energy for signification heat transfer and lead to the thermal wave propagation with a finite speed. The mathematical representation for the non-Fourier heat conduction is a

hyperbolic equation that included a wave propagation term. The heat transfer propagates at a finite speed instead of infinite speed that is the Fourier heat conduction.

During the past few years, the researcher had worked to remove the limitation of classical Fourier heat conduction law. The inspiration for this research was to eliminate the inconsistency of an infinite thermal wave speed which is in contradiction with Einstein's theory of relativity and thus provide a theory to explain the experimental data on second sound' in liquid and solid helium at low temperatures (Brown, Chung, & Matthews, 1966; Chester, 1963). In addition, in the case of low temperature, non-Fourier theories have attracted more attention in engineering sciences, because of their applications in high heat flux conduction, short time behaviour as found, for example, in laser-material interaction. As a common rule, when very fast transient heat conduction are encountered, the classical Fourier law of conduction is no longer accurate and non-Fourier effects become significant. Technical examples range from microwave heating, thermal investigations of electronic chips, e.g. ICs, and generally speaking, when extremely short duration or very high frequency or quite high heat flux densities or source terms exist. The non-Fourier heat conduction equation with dual phase lag has shown in Equation (2.11).

$$Q(r, t + \kappa_a) = -K_c \nabla \theta(r, t + \kappa_b) \quad (2.11)$$

where κ_b is the phase delay of longitudinal temperature gradient in regard to local temperature and κ_a is the phase delay of heat flux in regard to local temperature.

2.5.4 Three Phase Lag (TPL) heat conduction model

There are numerous parabolic and hyperbolic theories which define the heat conduction, the latter also being called theories of second sound, where the propagation of heat is demonstrated with finite propagation speed, in contrast to the classical model using

Fourier's law leading to infinite propagation speed of heat signals, see the surveys by Chandrasekharaiah (Chandrasekharaiah, 1998) or Hetnarski and Ignaczak (R. B. Hetnarski & Ignaczak, 1999) (R. Hetnarski & Ignaczak, 2000). In recent times, there have been considered the dual-phase-lag heat equations which were proposed by Tzou (L. Wang & Xu, 2002) and investigated by Quintanilla and Racke (R. Quintanilla, 2002; Ramón Quintanilla & Racke, 2006, 2007) and Wang et al. (L. Wang & Xu, 2002; L. Wang, Xu, & Zhou, 2001). There were described some models for the conduction of heat in the thermo-mechanical context. We can recall the models proposed by Hetnarski and Ignaczak (R. B. Hetnarski & Ignaczak, 1999). It is worth noting that, the model proposed by Tzou contains the theories of Lord and Shulman, Green and Lindsay as particular cases. When several orders of approximation are considered in Tzou's theory the classical theory of Cattaneo is obtained. However, the theories proposed by Green and Naghdi (Green & Naghdi, 1992) cannot be obtained from this point of view. Recently Roy (Choudhuri, 2007) has suggested a theory with three phase-lag model which is able to contain all the previous theories at the same time. The basic equation is,

$$q(r, t + \kappa_a) = -\left(K_c \nabla \theta(r, t + \kappa_b) + K_c^* \nabla v(r, t + \kappa_v)\right) \quad (2.12)$$

2.6 Summary

Non-Fourier heat conduction model is mixed derivative of time space which makes it difficult to tackle numerically. A number of iterative and moment matching based method can be found to analyse the heat conduction. In earlier decades, the thermal analyses have been done by using traditional iterative method. These iterative methods were undeniably very precise, but these methods are computationally expensive. Model based parameter estimation (MBPE) was made notorious to abate the computational time (Burke, Miller, Chakrabarti, & Demarest, 1989). In 1990, moment matching based method namely asymptotic waveform evaluation (AWE) was presented [2], which is a

special case of MBPE technique; and they are competent to show that, AWE method is at least 3.33 times faster than the conventional iterative based numerical methods. Unfortunately, the AWE moment matching is ill-conditioned, because AWE technique is incompetent to forecast the delay and initial high frequencies in an accurate manner(Loh et al., 2007). Then in Lanczos process was developed (Lanczos, 1950); and in this process, the linear systems are transformed into Pade approximation deprived of forming ill-conditioned moments.

But, if the systems are non-linear, researcher either can elucidate the problem by using ill-conditioned AWE technique or they have to convert the non-linear system into linear system. If they linearize the problems, either higher order term deserted or they should be familiarized superfluous degree of freedoms. To evade all those complications, a technique was introduced, entitled well-conditioned asymptotic waveform evaluation (WCAWE) (Slone, Lee, & Lee, 2003). Using WCAWE method, moment matching process does not disregard higher order term and also avoids extra degree of sovereignty for non-linear systems. In WCAWE method, they acquaint with two correction terms to confiscate ill-condition of AWE moment matching and this method was well-recognized to solve the frequency domain finite element problem exclusively for electromagnetic problems, where the simulation was carried out for different types of antennas. In WCAWE method, Z matrix was picked randomly to find out the correction terms. In recent years, WCAWE method is used to solve the most challenging Helmholtz finite element model(Souza Lenzi, Lefteriu, Beriot, & Desmet, 2013).

The objectives of the present work, are to deliberate about Fourier and non-Fourier heat conduction problems for diverse boundaries conditions. Already a lot of research has been done in previous decades. All of them used iterative based numerical method to analyse the

Fourier and non-Fourier heat conduction equation with different initial and boundary conditions (Baumeister & Hamill, 1969,1971; D.Tang & Araki,1996,2000).

In recent years researcher has started to use moment matching based method. In AWE method, the non-Fourier heat conduction models are needed to be converted into a linear equation (P. Liu et al., 2006; M. S. Rana, Jeevan, Harikrishnan, & Reza, 2014). In this method, higher order term is deserted during the transformation of linear equation. Hence, the technique is not capable to forecast the tangible temperature responses. Recently, Tikhonov based well condition scheme was proposed for fast transient thermal analysis of non-Fourier heat conduction. The technique successfully approximates the temperature responses for single boundary condition, as reported in our paper(S. Rana, Kanesan, Reza, & Ramiah, 2014).

However, the method cannot predict the temperature responses in case of different boundary conditions because the algorithm might breakdown in any specific situation. Therefore, in the current work, we propose a TWCAWE method to investigate the Fourier and non-Fourier heat conduction in different boundary conditions, which implanted with Tikhonov regularization technique to enrich the immovability (Mishra & Roy, 2007; Neumaier, 1998). In proposed TWCAWE model, no need to renovate non-Fourier heat conduction equation into linear equation. In the current study, we are capable to find out the Z matrix mathematically instead of choosing randomly, which assists to find out the correction term efficiently. The results attained from TWCAWE method precisely matched with Runge-Kutta (R-K) results and also competent to remove all instabilities of AWE.

3 CHAPTER 3: ANALYTICAL TECHNIQUES FOR HEAT CONDUCTION

3.1 Finite element model

3.2 Fundamental concept

The finite element model (FEM) is a numerical technique for solving problems, which are described by partial differential equations or can be formulated as functional minimization. A domain of interest is represented as an assembly of finite elements. Approximating the functions in finite elements is determined in terms of nodal values of a physical field which is required. In FEM, a continuous physical problem is distorted into a discretized finite element problem with unknown nodal values. Values inside finite elements can be recovered using nodal values. The main features of the FEM are worth to be stated as below:

- FEM can readily handle very complex geometry: The heart and power of the FEM.
- It able to handle a wide variety of engineering problems (such as solid mechanics, dynamics, heat problems, fluids, electrostatic problems).
- FEM can handle complex restraints (Indeterminate structures can be solved).
- It also able to handle the complex loading (Nodal load (point loads), Element load (pressure, thermal, inertial forces, Time or frequency dependent loading).

3.2.1 Working steps of Finite Element Model

The step by step working procedures of FEM are shown in Figure 3.1 and we also afford a short description of every step in below.

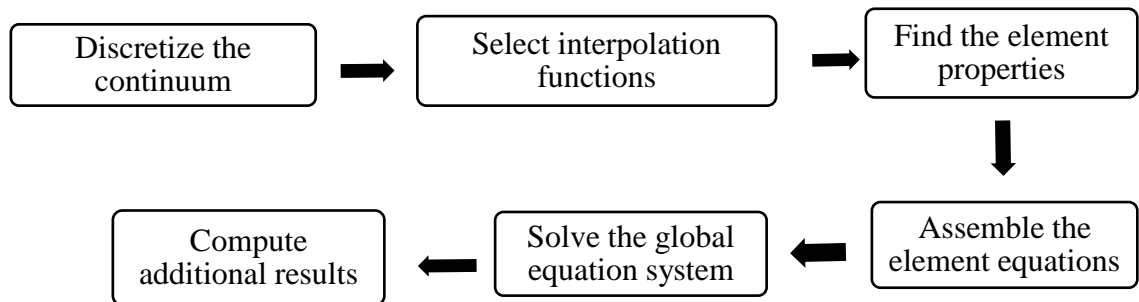


Figure 3.1: Working phase of Finite Element Model

- Discretize the continuum

The first step is to divide a solution region into finite elements. The finite element mesh is typically generated by a pre-processor program. The description of mesh consists of several arrays, main of which are nodal coordinates and element connectivity.

- Select interpolation functions

Interpolation functions are used to interpolate the field variables over the element. Often, polynomials are selected as interpolation functions. The degree of the polynomial depends on the number of nodes assigned to the element.

- Find the element properties

The matrix equation for the finite element should be established, which is relates the nodal values of the unknown function to other parameters. For this task different approaches can be used; the most convenient are: the variational approach and the Galerkin method.

- Assemble the element equations

To find the global equation system for the whole solution region, we must assemble all the element equations. In other words, we must combine local element equations for all elements used for discretization. Elements connectivities are used for the assembly process. Before solution, boundary conditions (which are not accounted in element equations) should be imposed.

- Solve the global equation system

The finite element global equation system is typically sparse, symmetric and positive definite. Direct and iterative methods can be used for solution. The nodal values of the sought function are produced as a result of the solution.

- Compute additional results

In many cases, we need to calculate additional parameters. For example, in mechanical problems strains and stresses are of interest in addition to displacements, which are obtained after solution of the global equation system.

Figure 3.2 shows combine triangular and rectangular mesh. This figure also shows FEM meshing and nodes. By using FEM meshing, we can use different boundary conditions as our required.

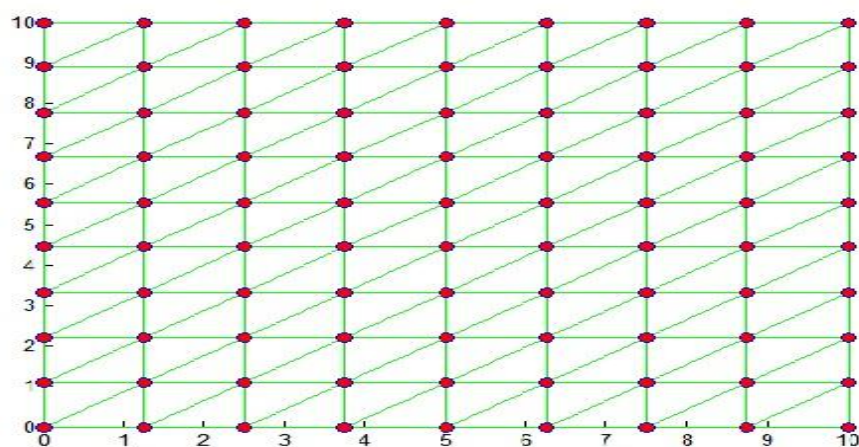


Figure 3.2: Triangular and rectangular mesh for two dimensional slab

3.2.2 Fundamental equation of FEM

Many engineering problems can be stated by governing equations and boundary conditions. Consider a governing and boundary equations are following:

$$L(\omega) + f = 0$$

$$B(\omega) + g = 0$$

FEM approximation converts above equation into a set of simultaneous algebraic equation as follows:

$$[K]\{u\} = \{F\}$$

Where, [K] is property, {u} is behavior and F(Horowitz) is action. This is the fundamental equation of FEM. This fundamental equation is applicable for solid mechanics, dynamics, heat problems, fluids, electrostatic problems. In different cases property, behaviour and actions changes. In this dissertation, we have used FEM for heat problems.

3.2.3 Finite element equations for heat transfer

Let us consider an isotropic body with temperature dependent heat transfer. A basic equation of heat transfer has the following appearance:

$$-\left(\frac{\partial q_x}{\partial x} + \frac{\partial q_y}{\partial y} + \frac{\partial q_z}{\partial z}\right) + Q = \rho c \frac{\partial T}{\partial t} \quad (3.1)$$

Here q_x , q_y and q_z are components of heat flow through the unit area; $Q = Q(x; y; z; t)$ is the inner heat generation rate per unit volume; ρ is material density; c is heat capacity; T is temperature and t is time. According to the Fourier's law, the components of heat flow can be expressed as follows

$$q_x = -K_c \frac{\partial T}{\partial x}$$

$$q_y = -K_c \frac{\partial T}{\partial y}$$

$$q_z = -K_c \frac{\partial T}{\partial z}$$

Where K_c is the thermal conductivity coefficient of the media. Substitution of Fourier's relations gives the following basic heat transfer equation is shown in below:

$$\left(\frac{\partial}{\partial x} \left(K_c \frac{\partial T}{\partial x} \right) + \frac{\partial}{\partial y} \left(K_c \frac{\partial T}{\partial y} \right) + \frac{\partial}{\partial z} \left(K_c \frac{\partial T}{\partial z} \right) \right) + Q = \rho c \frac{\partial T}{\partial t} \quad (3.2)$$

It is assumed that boundary conditions can be of the following types:

i) Specified temperature

$$T_s = T(x; y; z; t) \text{ on } S_1$$

ii) Specified heat flow

$$q_x n_x + q_y n_y + q_z n_z = h(T_s - T_e) \text{ on } S_3$$

iii) Radiation

$$q_x n_x + q_y n_y + q_z n_z = \sigma \varepsilon T_s^4 - \alpha q_r \text{ on } S_4$$

Where σ is the Stefan-Boltzmann constant; ε is the surface emission coefficient; α is the surface absorption coefficient and q_r is incoming heat flow per unit surface area.

For transient problems it is necessary to specify a temperature field for a body at the time $t = 0$, that is:

$$T(x; y; z; 0) = T_0(x; y; z)$$

3.3 Mathematical formulation for DPL heat conduction model

D.Y. Tzou proposed a non-Fourier heat transfer model that contains of two phase delay denoted by Equation (3.3). Due to the presence of phase delay this model able to describe these distinct situation of heat conduction, e.g., near the absolute zero temperature and extreme thermal gradient and also able to eradicate the dimness of classical heat conduction model.

$$Q(r, t + \kappa_a) = -K_c \nabla \phi(r, t + \kappa_b) \quad (3.3)$$

where, κ_b is the phase delay of longitudinal temperature gradient in regard to local temperature and κ_a is the phase delay of heat flux in regard to local temperature.

The DPL heat conduction model denoted by Equation (3.3) promises both phase delay κ_a and κ_b for fast heat transfer. The model is comprehensive into a standardized two-dimensional hyperbolic equation specified by Equation (3.4).

$$\frac{\partial^2 \phi}{\partial \varepsilon^2} + \frac{\partial^2 \phi}{\partial \psi^2} + Z_b \frac{\partial^3 \phi}{\partial \beta \partial \varepsilon^2} + Z_b \frac{\partial^3 \phi}{\partial \beta \partial \psi^2} = \frac{\partial \phi}{\partial \beta} + Z_a \frac{\partial^2 \phi}{\partial \beta^2} \quad (3.4)$$

where,

$$\phi = \frac{\theta - \theta_0}{\theta_w - \theta_0}, \quad \beta = \frac{t}{l^2/\sigma}, \quad \varepsilon = \frac{x}{l}, \quad \psi = \frac{y}{h}, \quad Z_a = \frac{\kappa_a}{l^2/\sigma}, \quad Z_b = \frac{\kappa_b}{l^2/\sigma}$$

β is standardized time, Z_b is standardized phase delay for temperature gradient, Z_a is standardized phase delay for heat flux. The length and width are given by l and h correspondingly, while σ is thermal diffusivity.

Finite element model (FEM) is sturdy technique as its able explains multi-dimensional and diverse types of problems. FEM meshing was carried out using rectangular element with nodes i, j, k and m . FEM based on Galerkin's weighted residual technique is pragmatic on Equation (3.4) to attain Equation (3.5)(Loh et al., 2007).

$$\int_A [N]^T \left[\frac{\partial^2 \phi}{\partial \varepsilon^2} + \frac{\partial^2 \phi}{\partial \psi^2} + Z_b \frac{\partial^3 \phi}{\partial \beta \partial \varepsilon^2} + Z_b \frac{\partial^3 \phi}{\partial \beta \partial \psi^2} - \frac{\partial \phi}{\partial \beta} - Z_a \frac{\partial^2 \phi}{\partial \beta^2} \right] \partial \varepsilon \partial \psi = 0 \quad (3.5)$$

Elemental matrices can be instigated for any type of model by using Equation (3.5).

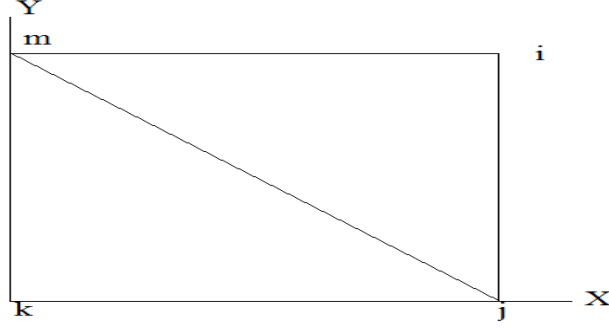


Figure 3.3: A two dimensional single element

Consider a rectangular slab with node i , j , k and m . By applying weak formulation to Equation (3.5), the elemental contribution is obtained as Equation (3.6). The below equation denoted by 3.6 will helps to calculate the two dimensional elemental metrics.

$$\begin{aligned} & [N]^T \frac{\partial \phi}{\partial \varepsilon} \Big|_j^k + [N]^T \frac{\partial \phi}{\partial \psi} \Big|_k^m + Z_b [N]^T \frac{\partial \phi}{\partial \varepsilon} \Big|_j^k + Z_b [N]^T \frac{\partial \phi}{\partial \psi} \Big|_k^m - \int_j^k \frac{\partial [N]^T}{\partial \varepsilon} \frac{\partial \phi}{\partial \varepsilon} dA - \int_k^m \frac{\partial [N]^T}{\partial \psi} \frac{\partial \phi}{\partial \psi} dA \\ & - \int_j^k Z_b \frac{\partial [N]^T}{\partial \varepsilon} \frac{\partial \phi}{\partial \varepsilon} dA - \int_k^m Z_b \frac{\partial [N]^T}{\partial \psi} \frac{\partial \phi}{\partial \psi} dA - \int_j^k (N_k \dot{\phi} + Z_a N_k \ddot{\phi}) d\zeta d\zeta = 0 \end{aligned} \quad (3.6)$$

3.4 Different analytical technique for dual phase lag heat conduction

A number of analytical techniques can be found to analyze the non-Fourier heat conduction with DPL model. Some analytical techniques are based on iteration such as Runge-Kutta. The results obtained from traditional iterative techniques are accurate and precise. Unfortunately, these traditional techniques are computationally expensive. To reduce computational time, moment matching based technique was introduced such as AWE, WCAWE. All these techniques are described in below.

3.4.1 Runge- Kutta Method

In numerical analysis, the Runge–Kutta is an important family of implicit and explicit iterative methods, which are used in temporal discretization for the approximation of solutions of ordinary differential equations. The 4th-order RungeKutta method is a sample of the slope is made at the mid-point on the interval, as well as the end points, and a weighted average is taken, placing more weight on the slope at the mid-point. It should be noted that, Runge-Kutta refers to an entire class of IVP solvers, which includes Euler's method and Heun's method. The results accuracy of Runge-Kutta method is strongly depends on selection of step size. Small step size gives good results; but takes more simulation time.

The Runge-Kutta algorithm may be very crudely described as "Heun's Method on steroids." It takes to extremes the idea of correcting the predicted value of the next solution point in the numerical solution. Without further ado, using the same notation, here is a summary of the fourth order Runge-Kutta methods are shown in below Table 3.1:

Table 3.1: Fourth order Runge-Kutta method

$$x_{n+1} = x_n + h$$
$$y_{n+1} = y_n + \frac{1}{6}(k_1 + 2k_2 + 2k_3 + k_4)$$

where,

$$k_1 = hf(x_n, y_n)$$
$$k_2 = hf(x_n + h/2, y_n + k_1/2)$$
$$k_3 = hf(x_n + h/2, y_n + k_2/2)$$
$$k_4 = hf(x_n + h, y_n + k_3)$$

First we note that, the Runge-Kutta method iterates the x -values by simply adding a fixed step-size of h at each iterations. The y -iteration formula is far more interesting. It is

a weighted average of four values— k_1 , k_2 , k_3 , and k_4 . Visualize distributing the factor of $1/6$ from the front of the sum. Doing this we see that k_1 and k_4 are given a weight of $1/6$ in the weighted average, whereas k_2 and k_3 are weighted $1/3$, or twice as heavily as k_1 and k_4 . (As usual with a weighted average, the sum of the weights $1/6$, $1/3$, $1/3$ and $1/6$ is 1.).

k_1 , we may recognize as the quantity, $hf(x_n, y_n)$, is simply Euler's prediction for what we've previously called Δy —the vertical jump from the current point to the next Euler-predicted point along the numerical solution.

k_2 we have never seen before. Notice the x -value at which it is evaluating the function $f(x_n + h/2)$ lies halfway across the prediction interval. $y_n + k_1/2$ is the current y -value plus half of the Euler-predicted Δy that we just discussed as being the meaning of k_1 . So this too is a halfway value, this time vertically halfway up from the current point to the Euler-predicted next point. To summarize, then, the function f is being evaluated at a point that lies halfway between the current point and the Euler-predicted next point. Recalling that the function f gives us the slope of the solution curve, we can see that evaluating it at the halfway point just described, i.e. $f(x_n + h/2, y_n + k_1/2)$, gives us an estimate of the slope of the solution curve at this halfway point. Multiplying this slope by h , just as with the Euler Method before, produces a prediction of the y -jump made by the actual solution across the whole width of the interval, only this time the predicted jump is not based on the slope of the solution at the left end of the interval, but on the estimated slope halfway to the Euler-predicted next point.

k_3 has a formula which is quite similar to that of k_2 , except that where k_1 used to be, there is now a k_2 . Essentially, the f -value here is yet another estimate of the slope of the solution at the "midpoint" of the prediction interval. This time, however, the y -value of the midpoint is not based on Euler's prediction, but on the y -jump predicted already

with k_2 . Once again, this slope-estimate is multiplied by h , giving us yet another estimate of the y -jump made by the actual solution across the whole width of the interval.

k_4 evaluates f at $x_n + h$, which is at the extreme right of the prediction interval. The y -value coupled with this, $y_n + k_3$, is an estimate of the y -value at the right end of the interval, based on the y -jump just predicted by k_3 . The f -value thus found is once again multiplied by h , just as with the three previous k_i , giving us a final estimate of the y -jump made by the actual solution across the whole width of the interval.

In summary, then, each of the k_i gives us an estimate of the size of the y -jump made by the actual solution across the whole width of the interval. The first one uses Euler's Method, the next two use estimates of the slope of the solution at the midpoint, and the last one uses an estimate of the slope at the right end-point. Each k_i uses the earlier k_i as a basis for its prediction of the y -jump.

This means that the Runge-Kutta formula for y_{n+1} , namely:

$$y_{n+1} = y_n + (1/6)(k_1 + 2k_2 + 2k_3 + k_4)$$

is simply the y -value of the current point plus a weighted average of four different y -jump estimates for the interval, with the estimates based on the slope at the midpoint being weighted twice as heavily as the those using the slope at the end-points.

3.4.2 Asymptotic Waveform Evaluation

Asymptotic waveform evaluation (AWE) technique, which has been used for fast transient circuit simulation, is based on the concept of approximating the original system with a reduced order system. The inspiration of AWE came from Horowitz et al (Horowitz, 1983) where RC-tree networks were estimated using efficient Elmore delay approach. However, these estimates were not always accurate. A second breakthrough

came from the work of McCormick (McCormick, 1989), in which he has used the interconnect circuit moments to form a lower order circuit models to predict transient responses accurately. The efforts of these authors lead to the formalization and generalization of AWE algorithms (Pillage & Rohrer, 1990). For more than a decade, extensive works on AWE has been carried out. AWE has been successfully applied for fast transient circuit simulation (T. K. Tang & Nakhla, 1992). AWE also has a lot of successes in electromagnetic simulations.

However, there are some papers available on the application of AWE in transient thermal simulation. Liu et al. (D.-G. Liu, Phanilatha, Zhang, & Nakhla, 1995) have published the first paper on thermal analysis of PCB using AWE scheme, but the details of incorporating the initial conditions were not addressed. Then, Ooi et al. (Ooi et al., 2003a) has successfully extended the AWE algorithm to incorporate the initial conditions. They created a generalized formulation using the concept of zero state response and zero input response, which is used in control system. However, Ooi et al. [9] did not address the inherent numerical instability of AWE, which may yield incorrect solutions. Both papers also only focused on solving Fourier heat conduction equation with AWE. In contrast, AWE is actually approximating the original system with reduced order system and thus, it is a few orders faster than conventional iterative solvers in term of computational time. It is also independent of time step because it produces the transient solutions in a form of equation, rather than numerical solutions at every increment of time step. AWE is also capable of producing local solution because it can obtain the solution for each node independently and thus further reducing the amount of computational time. However, the drawback of AWE is that the moment matching process in AWE is inherently ill-conditioned and thus may produce unstable response even for stable system. Higher order approximation will lead to a more accurate solution but not always guarantee a stable solution.

3.4.2.1 AWE moments matching

The governing equation for non-dimensionalized two-dimensional Fourier heat conduction is a parabolic equation as shown by Equation (3.4). After discretization of Equation (3.4) with Galerkin's weighted residual method, a set of first order linear differential equations is obtained as given by Equation (3.6). The detailed formulations of Eq. (3.6) can be obtained from Sienkiewicz (Loh et al., 2007; Zienkiewicz & Taylor, 2000).

$$D\ddot{\theta} + V\dot{\theta} + K\theta = F(t) \quad (3.6)$$

Finally element matrices derived from above equation (3.6) for triangular and rectangular meshing that shown in below

For triangular mesh the elemental matrixes are,

$$D = \frac{Z_a \bar{A}}{12} \begin{bmatrix} 2 & 1 & 1 \\ 1 & 2 & 1 \\ 1 & 1 & 2 \end{bmatrix}$$

$$V = \frac{\bar{A}}{12} \begin{bmatrix} 2 & 1 & 1 \\ 1 & 2 & 1 \\ 1 & 1 & 2 \end{bmatrix} + \frac{Z_b}{4\bar{A}} \begin{bmatrix} N_j^2 & N_j N_k & N_j N_m \\ N_j N_k & N_k^2 & N_k N_m \\ N_j N_m & N_k N_m & N_m^2 \end{bmatrix} + \frac{Z_b}{4\bar{A}} \begin{bmatrix} N_j^2 & N_j N_k & N_j N_m \\ N_j N_k & N_k^2 & N_k N_m \\ N_j N_m & N_k N_m & N_m^2 \end{bmatrix}$$

$$K = \frac{1}{4\bar{A}} \begin{bmatrix} N_j^2 & N_j N_k & N_j N_m \\ N_j N_k & N_k^2 & N_k N_m \\ N_j N_m & N_k N_m & N_m^2 \end{bmatrix} + \frac{1}{4\bar{A}} \begin{bmatrix} N_j^2 & N_j N_k & N_j N_m \\ N_j N_k & N_k^2 & N_k N_m \\ N_j N_m & N_k N_m & N_m^2 \end{bmatrix}$$

For rectangular mesh the elemental matrixes are,

$$D = \frac{Z_a \bar{A}}{36} \begin{bmatrix} 4 & 2 & 1 & 2 \\ 2 & 4 & 2 & 1 \\ 1 & 2 & 4 & 2 \\ 2 & 1 & 2 & 4 \end{bmatrix}$$

$$V = \frac{\bar{A}}{36} \begin{bmatrix} 4 & 2 & 1 & 2 \\ 2 & 4 & 2 & 1 \\ 1 & 2 & 4 & 2 \\ 2 & 1 & 2 & 4 \end{bmatrix} + \frac{Z_b}{6\bar{A}} \begin{bmatrix} N_i^2 & N_i N_j & N_i N_k & N_i N_m \\ N_i N_j & N_j^2 & N_j N_k & N_j N_m \\ N_i N_k & N_j N_k & N_k^2 & N_k N_m \\ N_i N_m & N_j N_m & N_k N_m & N_m^2 \end{bmatrix} + \frac{Z_b}{6\bar{A}} \begin{bmatrix} N_i^2 & N_i N_j & N_i N_k & N_i N_m \\ N_i N_j & N_j^2 & N_j N_k & N_j N_m \\ N_i N_k & N_j N_k & N_k^2 & N_k N_m \\ N_i N_m & N_j N_m & N_k N_m & N_m^2 \end{bmatrix}$$

$$K = \frac{1}{6\bar{A}} \begin{bmatrix} N_i^2 & N_i N_j & N_i N_k & N_i N_m \\ N_i N_j & N_j^2 & N_j N_k & N_j N_m \\ N_i N_k & N_j N_k & N_k^2 & N_k N_m \\ N_i N_m & N_j N_m & N_k N_m & N_m^2 \end{bmatrix} + \frac{1}{6\bar{A}} \begin{bmatrix} N_i^2 & N_i N_j & N_i N_k & N_i N_m \\ N_i N_j & N_j^2 & N_j N_k & N_j N_m \\ N_i N_k & N_j N_k & N_k^2 & N_k N_m \\ N_i N_m & N_j N_m & N_k N_m & N_m^2 \end{bmatrix}$$

The concept of AWE is to approximate the original response of a system with a reduced order system. Figure 1 shows the flow of AWE algorithm, which can be categorized into three major steps. The response of a system can be represented by a polynomial equation in s-domain, where the coefficients of this polynomial are known as the moments (McCormick, 1989; Pillage & Rohrer, 1990). In moment generation, the moments are determined for zero state response (ZSR) and zero input response (ZSR). The concept of ZSR and ZIR is used by Ooi et al. (Ooi et al., 2003b) to account for the boundary and initial conditions, respectively. In ZSR, the initial conditions of the system are assumed to be zero, while the forcing functions are assumed to be zero in ZIR. In moment matching, the order of the system response is reduced using Pade' approximation, and then further simplified to a set of partial fractions, where each partial fraction contains a pole and also a zero. Finally, each partial fraction is inverted Laplace back to time domain and summed up to provide the transient solution.

3.4.2.2 First order differential equation

Classical Fourier's law is based on diffusion model with assumption of infinite thermal wave propagation speed, which leads to simultaneous development of heat flux and temperature gradient. Classical Fourier's law also assumes that, instantaneous local thermal equilibrium occurs between electrons and phonons. In other words, classical Fourier's law dictates that, the thermal effect is felt instantaneously throughout the

system if the surface of a material is heated. The governing equation for non-dimensionalized two-dimensional Fourier heat conduction is a parabolic equation as shown below equation.

$$\frac{\partial^2 \theta}{\partial \delta^2} + \frac{\partial^2 \theta}{\partial \varepsilon^2} = \frac{\partial \theta}{\partial \beta} \quad (3.7)$$

Where, θ is the dimensionless temperature and β is the dimensionless time. The dimensionless distance x and y are represented by δ and ε , respectively. After discretization of Equation (3.7) with Galerkin's weighted residual method, a set of first order linear differential equations is obtained as given by Equation (3.8). The detailed formulations of Equation (3.8)

$$C\dot{\theta} + K\theta = f \quad (3.8)$$

Where, C is known as the capacitive matrix, while K is the conductivity matrix and f represents the load vector, which can be time-dependent or time-independent. Taking Laplace transform of Equation (3.8),

$$C(s\theta(s) - \theta(0)) + K\theta(s) = f$$

The system solution, $\theta(s)$ can be approximated by using polynomial equation in s -domain, as given by Equation (3.9).

$$T(s) = \sum_{n=0}^{\infty} M_n s^n \quad (3.9)$$

The moments, M_n , are the coefficients of Taylor series expansion about $s = 0$ (Maclaurin series). Moments are generated, respectively, for ZSR and ZIR by substituting Equation (3.9) into Equation (3.8) as following,

- Zero state response (ZSR)

In ZSR, the initial condition is assumed to be zero, $\theta(0) = 0$.

$$(Cs + K)(M_0 + M_1s + M_2s^2 + \dots + M_ns^n) = f \quad (3.9)$$

By equating the same powers of s, the moments are generated from Equation(3.10).

$$KM_0 = f$$

$$KM_n = -CM_{n-1} \text{ for } n=1,2,3,\dots,(2q-1) \quad (3.10)$$

- Zero input response (ZIR)

In ZIR, the forcing function is assumed to be zero, $f = 0$.

$$(Cs + K)(M_0 + M_1s + M_2s^2 + \dots + M_ns^n) = CT(0)$$

Again by equating the same powers of s, the moments are generated from Equation(3.11).

$$KM_0 = C\theta(0)$$

$$KM_n = -CM_{n-1} \text{ for } n=1,2,3,\dots,(2q-1) \quad (3.11)$$

3.4.2.3 Second order differential equation

For hyperbolic heat conduction equation as shown by Equation(3.3), it can be reduced to a set of second order differential equations using Galerkin's weighted residual method(Cheah, Seetharamu, Ghulam, Zainal, & Sundararajan, 2000; Prakash, Reddy, Das, Sundararajan, & Seetharamu, 2000) which mentioned in Equation (3.6).The Laplace of above equation (3.6) is shown in below:

$$D(s^2\theta(s) - s\theta'(0) - \theta(0)) + V(s\theta(s) - \theta(0)) + K\theta(s) = F$$

$$s^2D\theta(s) + s(V\theta(s) - D\theta'(0)) + K\theta(s) - (D + V)\theta(0) = F$$

The system solution, $\theta(s)$ can be approximated by using polynomial equation in s -domain, as given by following equation

$$\theta(s) = \sum_{n=0}^{\infty} M_n s^n$$

The moments, M_n , are the coefficients of Taylor series expansion about $s = 0$ (Maclaurin series)(McCormick, 1989; Pillage, Huang, & Rohrer, 1989; Pillage & Rohrer, 1990).

Similar as above, the ZSR and ZIR moment can be found as follows:

- Zero state response (ZSR)

In ZSR, the initial condition is assumed to be zero, $\theta(0)=0$ and $\theta'(0)=0$

$$s^2 D\theta(s) + s(V\theta(s) - D\theta'(0)) + K\theta(s) - (D + V)\theta(0) = F$$

$$(Ds^2 + Vs + K)(M_0 + M_1s + M_2s^2 + \dots + M_n s^n) = F$$

By equating the same powers of s , the moments are generated from below equation

$$KM_0 = F$$

$$KM_1 = -VM_0$$

$$KM_n = -(DM_{n-2} + VM_{n-1}) \text{ for } n = 2, 3, \dots, (2q-1) \quad (3.12)$$

- Zero input response (ZIR)

$$KM_0 = VT(0) + DT(0)$$

$$KM_1 = DT(0) - VM_0$$

$$KM_n = -(DM_{n-2} + VM_{n-1}) \text{ for } n = 2, 3, \dots, (2q-1) \quad (3.13)$$

3.4.2.4 Transient response

The nodal moments $[a]$ can be take out from global moment matrix for any random node i is

$$[a_n]_i = [\hat{V}]_i \quad (3.14)$$

The transient response for any random node i can be approximated by using Pade approximation, then supplementary streamlined to partial fractions(Pillage & Rohrer, 1990)as exposed as equations (3.115)-(3.17).

$$T_i(s) = a_0 + a_1s + a_2s^2 + \dots + a_n s^n \quad (3.15)$$

$$= \frac{\mathbf{d}_0 + \mathbf{d}_1s + \dots + \mathbf{d}_{s-1}s^{s-1}}{1 + \mathbf{c}_1s + \dots + \mathbf{c}_s s^s} \quad (3.16)$$

$$= \frac{r_1}{s - p_1} + \frac{r_2}{s - p_2} + \dots + \frac{r_q}{s - p_q} \quad (3.17)$$

Poles and Residues can be originated by resolving equations (3.18)-(3.20)

$$\begin{bmatrix} a_0 & a_1 & a_2 & \dots & a_{q-1} \\ a_1 & a_2 & a_3 & \dots & a_q \\ \dots & \dots & \dots & \dots & \dots \\ \dots & \dots & \dots & \dots & \dots \\ a_{q-1} & \dots & \dots & \dots & a_{2q-2} \end{bmatrix} \begin{bmatrix} c_q \\ c_{q-1} \\ \cdot \\ \cdot \\ c_1 \end{bmatrix} = - \begin{bmatrix} a_q \\ a_{q-1} \\ \cdot \\ \cdot \\ a_1 \end{bmatrix} \quad (3.18)$$

$$\sum_{i=1}^r c_i p^i + 1 = 0 \quad (3.19)$$

$$\begin{bmatrix} p_1^{-1} & p_2^{-1} & p_3^{-1} & \dots & p_q^{-1} \\ p_1^{-2} & p_2^{-2} & p_3^{-2} & \dots & p_q^{-2} \\ \cdot & \cdot & \cdot & \dots & \cdot \\ \cdot & \cdot & \cdot & \dots & \cdot \\ p_1^{-s} & p_2^{-s} & p_3^{-s} & \dots & p_q^{-s} \end{bmatrix} \begin{bmatrix} r_1 \\ r_2 \\ \cdot \\ \cdot \\ r_q \end{bmatrix} = - \begin{bmatrix} a_0 \\ a_1 \\ \cdot \\ \cdot \\ a_{q-1} \end{bmatrix} \quad (3.20)$$

The transient response at an arbitrary node, i is given by the sum of ZSR and ZIR in time domain,

$$T_i(t) = ZSR(t) + ZIR(t)$$

$$T_i(t) = \sum_{j=1}^s \frac{r_j}{p_j} (e^{p_j t} - 1) + \sum_{j=1}^s r_j (e^{p_j t}) \quad (3.21)$$

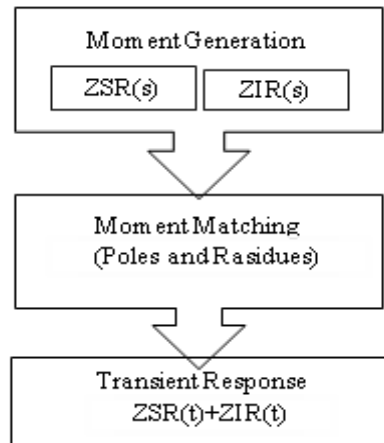


Figure 3.4: Flow of AWE algorithms

3.4.2.5 Numerical example

- Inherent instability of AWE in non-Fourier heat Conduction

AWE is used to model the transient non-Fourier heat conduction of two-dimensional slab subjected to instantaneous temperature rise on one edge, as shown in Figure 3.5. The dimensionless parameters used are $\delta = \epsilon = 1$ (size) and $Z_a = 0.05$. Z_b is taken at 0.0001 (wave-like). Without implementing any stability scheme, some arbitrary nodes are expected to have positive real poles and the solutions at these nodes are going to be

unstable and incorrect. As explained above, the generation of unstable positive real poles is due to the inherently ill-conditioned moment matching process in AWE. In this case, higher order approximation is also more prone to yielding unstable response, whereas lower order approximation will reduce the number of nodes with unstable response. There is no smooth and continuous trend for the nodal responses along the top edge of slab, and the solutions at some nodes are also fluctuating incorrectly as shown in Figure 3.5.

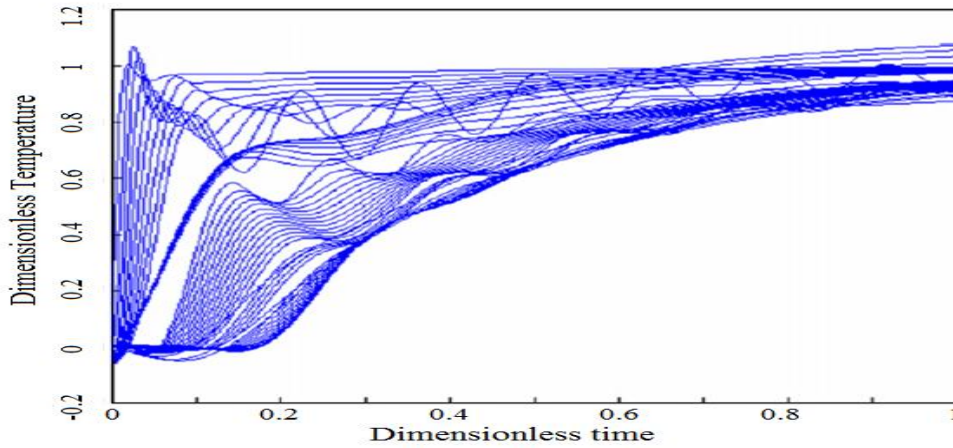


Figure 3.5: Dimensionless temperature distribution along the top edge of slab at $Z_b = 0.0001$

- AWE with partial pade

The moment matching process in AWE is inherently ill-conditioned, because Pade' approximation is well-known for yielding unstable poles. In the scope of finite element analysis, AWE can produce correct solutions for most of the nodes, but may yield incorrect solutions for some arbitrary nodes.

To further elaborate the weakness of Pade' approximation, consider a stable system, $H(s)$, with two negative value poles and it is to be approximated by a one pole system, $G(s)$ using Pade' approximation, as follows:

$$H(s) = \frac{r_1}{s - p_1} + \frac{r_2}{s - p_2} \text{ and } G(s) = \frac{\bar{r}}{s - \bar{p}} \quad (3.22)$$

With some mathematical manipulation, it can be shown that \bar{p} are related to the original poles and residues by Equation (3.22). \bar{p} has to be a negative value left-half plane pole in order to have a stable reduced order system, $G(s)$. However, as per Equation (3.22) \bar{p} can still be rendered to become a positive value right-half plane pole depending on the values of the residues (r_1 and r_2), even though both p_1 and p_2 are negative value left-half plane poles. The process of yielding undesirable positive poles is random, but it can be overcome by using the stability schemes.

The applied stability scheme does manage to suppress all unstable poles because there will be responses with very large magnitude if unstable poles exist. Yet, AWE solutions are still incorrect at some nodes because AWE fails to actually approximate the high frequency responses for nodes adjacent to the instantaneous temperature rise boundary condition, and thus causing the approximations for other nodes to deviate from the actual responses as well. In other words, AWE is incapable to fully represent the steep responses at some nodes since it is making use of only exponential to make approximation of the original response. Thus, this failure also renders the solutions at other nodes to be incorrect as well.

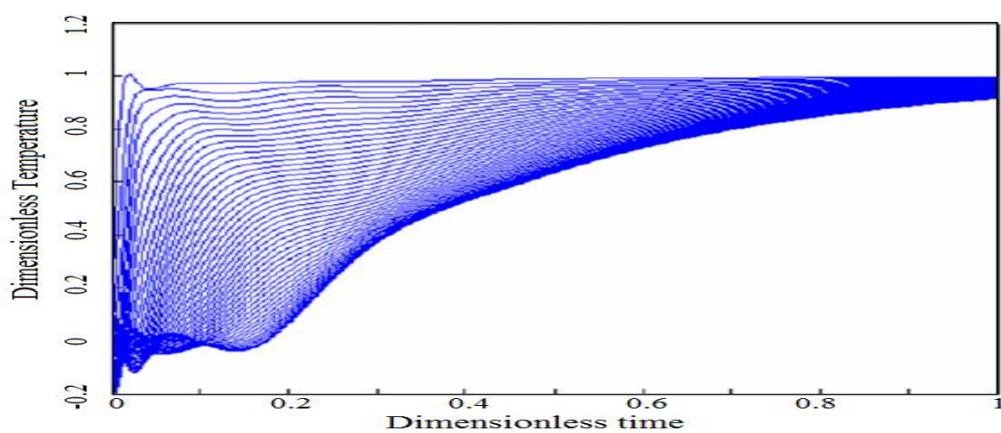


Figure 3.6: Dimensionless temperature distribution along the top edge of slab at $Z_T = 0.0001$ after applying partial Pade' approximation

In addition, partial Pade' approximation is also introduced to stabilize the AWE solutions for the case $Z_T = 0.0001$. In this stability scheme, the set of poles at an arbitrarily chosen node is used to approximate the responses of other nodes. In other words, this means that only the set of poles at an arbitrarily chosen node is calculated and it is used throughout the calculations of ZSR and ZIR for all other nodes. Usually, the node selected to approximate other nodes has high frequency response, and definitely it has to be stable. Therefore, it will eliminate the need to monitor the stability at every node. In this case, the node closest to the temperature load is chosen to approximate the temperature rise for other nodes along the top edge of slab, and only the poles at this chosen node are calculated. This node is chosen because it has the fastest temperature rise, or in other words, the response at this node is of high frequency. The temperature responses for nodes along the top edge of the slab are plotted on Figure 3.6. There is no unreasonable solution as compared to the former stability scheme because the poles used are selected from a chosen node, which is stable and also representing the correct response. This eliminates the generation of incorrect poles at some nodes (when using former stability scheme), which may renders the solutions to be incorrect. One way to determine a suitable node is to check the responses by using former stability scheme before applying partial Pade' approximation. The accuracy of this scheme has discussed Loh et al (Loh et al., 2007).

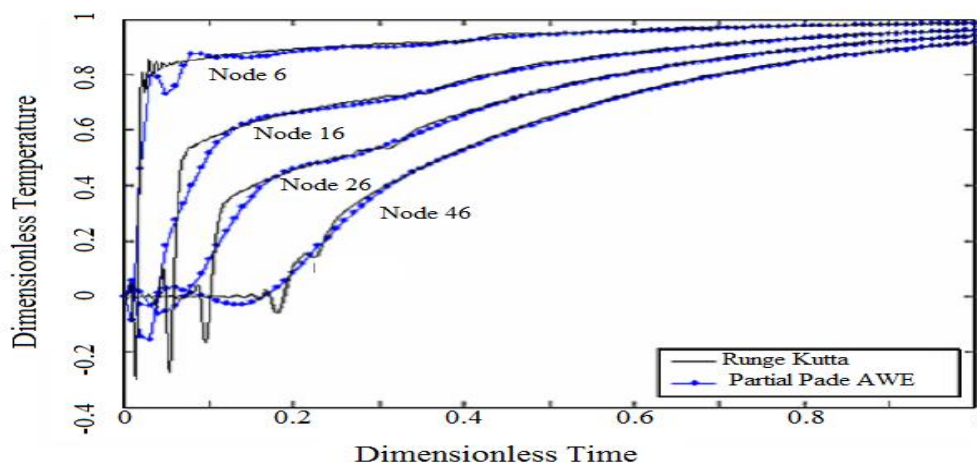


Figure 3.7: Comparison between AWE (after applying partial Pade' approximation) and Runge–Kutta for case $Z_b= 0.0001$

In addition, Figure 3.7 also shows that, AWE is not able to approximate the delay accurately since the response only consists of real and complex conjugate exponentials. This is because, to represent a pure delay, AWE is employing decaying sinusoids to artificially force the response close to zero for some initial period. This will lead to spurious ringing effects in the AWE waveforms as shown in Figure 3.5.

By analysing above results we can conclude that, AWE method is unable to approximate the temperature responses accurately due to presence of unstable positive real poles. On the other hand, AWE with partial pade also incapable to predict the delay accurately. In this dissertation, we have introduced some well-conditioned stability scheme to reduce complexity that is discussed in next chapter.

4 CHAPTER 4: AWE WITH WELL-CONDITIONED STABILITY SCHEME

In chapter 3, iteration based computational method Runge-Kutta (RK) and one moment matching based method have analyzed. Though, the results obtained from RK method are accurate but computationally expensive method. AWE method and partial pade AWE moment matching are inherently ill-conditioned. In this dissertation, we have found out the limitations of AWE method. To eliminate the limitations, we have some well-conditioned stability scheme. The stability schemes are discussed in below section.

4.1 Tikhonov regularization scheme

In many applications of linear algebra, necessary to find a good approximation 'x' to a vector $x \in \mathbb{R}^n$ satisfying an approximate equation $Kx \approx y$ with ill-conditioned or singular $K \in \mathbb{R}^{m \times n}$, given $y \in \mathbb{R}^m$. In all such situations, the vector $x = K^{-1}y$ (or in the full rank over determined case K^+y , with the pseudo inverse $K^+ = (K^*K)^{-1}K^*$), if it exists at all, is usually a meaningless bad approximation to x . So-called regularization techniques are needed to obtain meaningful solution estimates for such ill-posed problems.

In AWE moment matching, during the calculation of ZIR and ZSR denoted by Equation 3.12 and 3.13, need to take inverse of stiffness matrix K . AWE moments calculation are inaccurate due singularity problem of stiffness matrix. Tikhonov regularization technique has implements (Neumaier, 1998) to amend the stiffness matrix marginally in mandate to condense the volatility problem. Contemplate a well-condition approximation problem, $Kx \approx y$, the residual $\|Kx - y\|_2$ come to be minimum depend on the optimal of $x = (K^*K)^{-1}K^*y$. The singularity complaint of $(K^*K)^{-1}$ can be condense by adding a term which indicated in Equation (3.2)

$$x = (K * K + h_c^2 I)^{-1} K * y \quad (4.1)$$

Here, h_c is the regulation parameter which depends on order of equation, whereas I is the identical matrix. The family of this estimated inverse is defined by $C_h = (K * K + h_c^2 I)^{-1} K$. In TWCAWE, during moment calculation, inverse of K_0 matrix is supernumerary by C_h from WCAWE algorithm. Particulars of h_c and I can be found at (Neumaier, 1998).

4.2 AWE with Maximum Likelihood (ML) scheme

In AWE moment matching, some unstable positive poles are generated due to inherent ill-conditioned; which is responsible unstable temperature responses. To reduce this instability, a correction term J_u is introduced to obtain more stable responses. This correction term J_u is calculated from Z matrix as shown in equation (4.2). This Z matrix is nonsingular (P. Liu et al., 2006). The correction term J_u is obtained by using Maximum Likelihood (ML) from equation (4.2)

$$J_u(i) = \prod_{i=1}^r Z_{[i:i+2q+w-1, i:i+w-1]}^{-1} \quad (4.2)$$

Where, r is the number of node, w is order of equation and q is order of product. Now the new AWE poles and residues are calculated from equation (4.3) and (4.4) respectively,

$$P^*(i) = J_u(i)P(i) \quad (4.3)$$

$$R^*(i) = J_u(i)R(i) \quad (4.4)$$

4.3 T-WCAWE with Mass effect (ME) scheme

In partitioning of FEM, it was reported that the resulting interpolation function can lead to singular or ill-conditioned. This singularity occurs because some interpolations are linearly dependent and ill-condition occurs because the functions are very close to each other. To minimize this singularity and ill-condition, the mass matrix is changed by introducing a factor ‘ ζ ’ [18]. For small value of ζ , T-WCAWE with mass effect scheme reduces the effect of mass as given in equation (4.5).

$$D_s = (1 - \zeta)D_C + \zeta D_L \quad (4.5)$$

where

$$D_c = \frac{\kappa (\overline{\Delta x})^2}{36} \begin{bmatrix} 4 & 2 & 1 & 2 \\ 2 & 4 & 2 & 1 \\ 1 & 2 & 4 & 2 \\ 2 & 1 & 2 & 4 \end{bmatrix}$$

$$D_L = \frac{\kappa (\overline{\Delta x})^2}{4} \begin{bmatrix} 1 & & & \\ & 1 & & \\ & & 1 & \\ & & & 1 \end{bmatrix}$$

where κ is the grid aspect ratio and Δx is length of each element in X direction.

where $0 \leq \zeta \leq 1$ and D_c and D_L are consistent and row sum-lumped mass matrices respectively. The lumped mass matrix D_L has calculated using the total mass and allocating the lumped masses in the ratio of the diagonal element of the consistent mass matrix [19]. In this scheme D from equation (4) is replaced by new calculated D_s .

4.4 Numerical Example

The new AWE moments are calculated using above well-conditioned scheme. Then new poles and residues can be found. The final transient response can be found by using the equation 3.21. The working flow is same as the flowchart shown in Figure 3.4. Two well-conditioned scheme are embedded with Tikhonov regularization technique.

4.4.1 Observation of non-Fourier heat conduction

Figures 4.1-4.3 shows the temperature distribution for above rectangular slab considering different values of Z_T as 0.5, 0.05 and 0.0001 respectively. The temperature spectrum shown in Figures 4.1-4.3 are plotted by considering the node situated middle of the slab, all the responses are calculated by AWE using ML scheme. It is clear from the figure that, all temperature responses are continuous and accurate for different vale of Z_b . In this scheme, the individual poles and residues are used to calculate the individual temperature responses. So that, this scheme is accurately predict temperature distribution along the system. The initial high frequency and delay due to relaxation time of electron are clear in Figure 4.3 for $Z_b=0.0001$.

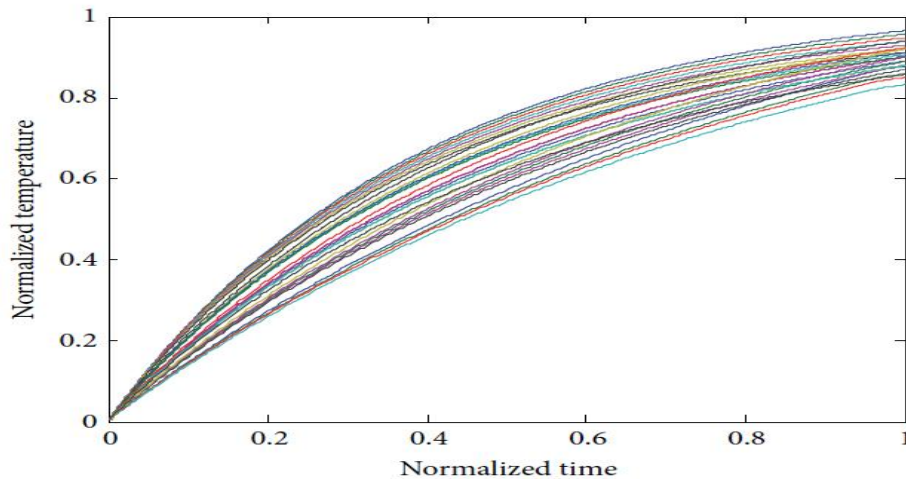


Figure 4.1: Normalized temperature response spectrum along centre of the slab in the case of $Z_b=0.5$

Though fourth order Runge-Kutta technique is slow, the results obtained from this method are more accurate due to its stability. Therefore our proposed model is compared with the results obtained by Runge-Kutta in Figure 4.4 and Figure 4.5.

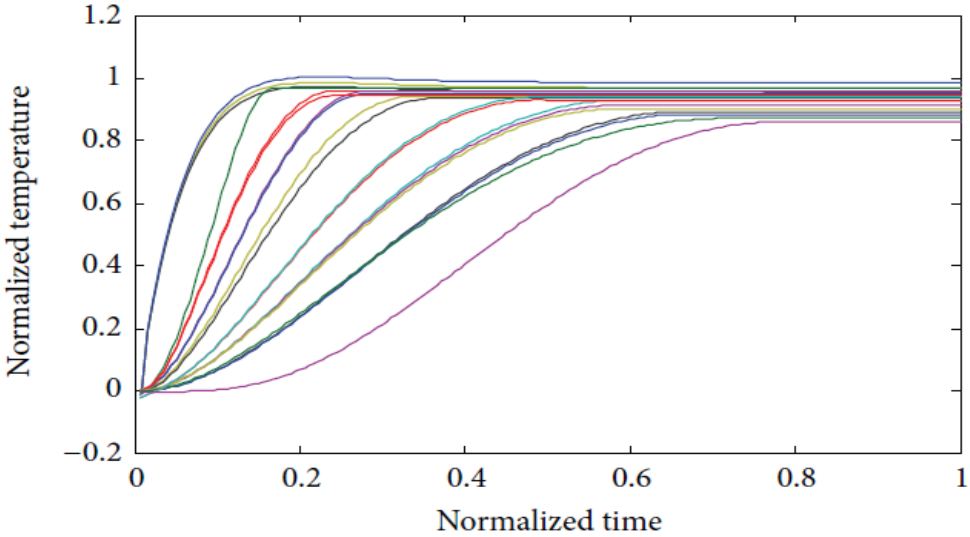


Figure 4.2: Normalized temperature response spectrum along centre of the slab in the case of $Z_b=0.05$

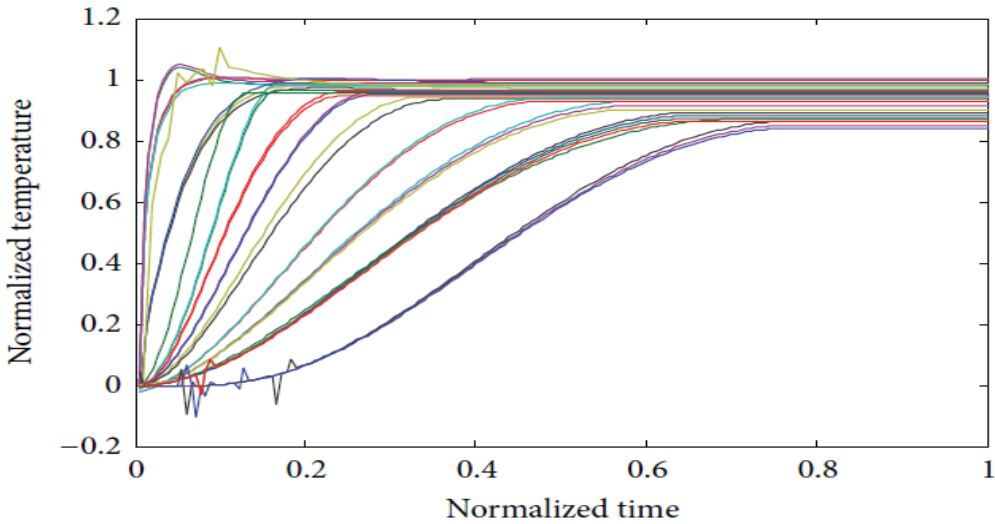


Figure 4.3: Normalized temperature response spectrum along centre of the slab for the case of $Z_b=0.0001$

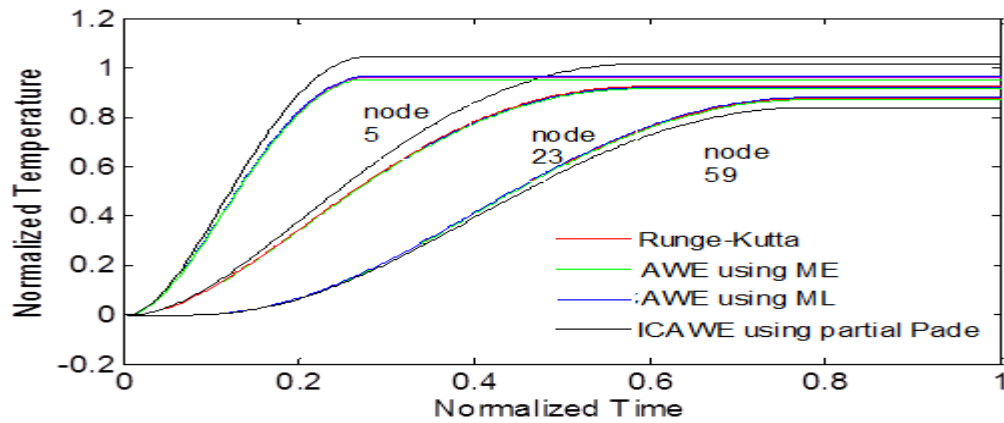


Figure 4.4: Comparison with T-WCAWE with ML, T-WCAWE with ME, Runge-Kutta and AWE using partial Pade in the case of $Z_b=0.05$

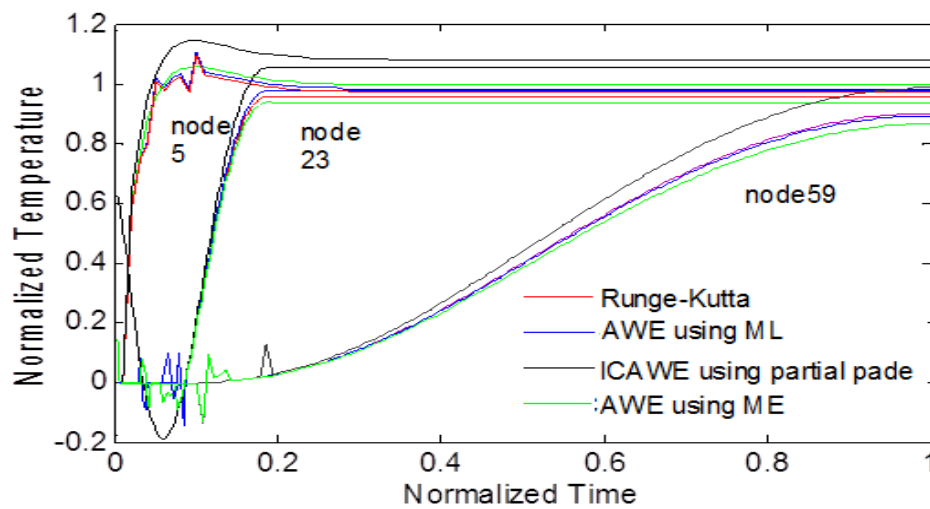


Figure 4.5: Comparison of T-WCAWE with ML, T-WCAWE with ME, Runge-Kutta and AWE with partial Pade for the case of $Z_b=0.0001$.

To show the accuracy of our proposed model, we compared both schemes, AWE with ML and AWE with ME against AWE using partial Pade and Runge-Kutta as shown in Figure 4.4. The comparison have been presented with $Z_b=0.05$. The temperature behavior obtained from both scheme of AWE is similar as Runge-Kutta. Partial pade AWE, however is unable predict the temperature behavior as Runge-Kutta. In partial pade AWE, arbitrarily chosen poles and residues are used to approximate the temperature behavior for whole system. Hence, this method was unable to calculate the

temperature behavior for other nodes. On the other hand, both schemes of AWE model use its own poles and residue to calculate the temperature behavior.

The comparison between our proposed two schemes is shown in Figure 4.5, where $Z_b=0.0001$. AWE with ME is able to calculate the delay and high frequency, but the temperature behavior deviates from Runge-Kutta results. On the other hand, the temperature behavior obtained from AWE with ML is in close proximity with Runge-Kutta.

To bring out the effectiveness of employing Tikhonov technique, we have performed another comparison in Figure 4.6 in the case of $Z_b=0.0001$. This figure shows that the temperature behavior obtained from AWE technique largely deviate from Runge-Kutta behavior. In AWE model, unstable poles makes moment matching process ill conditioned.

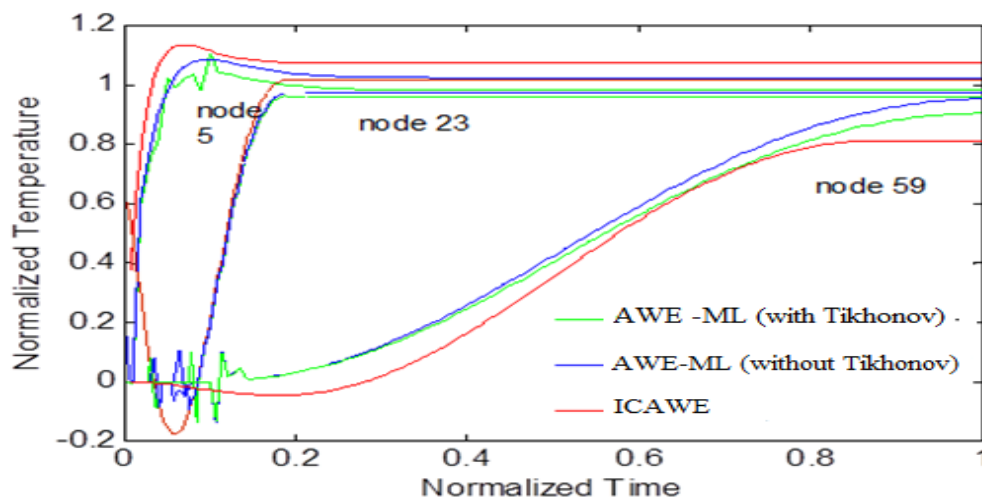


Figure 4.6: Comparison of AWE-ML (with Tikhonov), AWE-ML (without Tikhonov) and ICAWE (without Tikhonov) for $Z_b=0.0001$

The results obtained from AWE-ML without Tikhonov model are also not similar to AWE-ML using Tikhonov due to singularity problem of stiffness matrix. The error is compounded during the moment calculation and it becomes more evident for higher

order moment calculation. This causes AWE-ML without Tikhonov to be unstable and thus generating inaccurate initial high frequency responses compared to AWE-ML with Tikhonov making it difficult to observe the delay. The model developed in present work, AWE-ML with Tikhonov removed the singularity problem. This is carried out by adding new term based on Tikhonov regulation technique shown in Equation 4.2. The temperature behavior obtained by using AWE with ML is similar and close to Runge-Kutta shown in Figure 4.6. The model proposed in the present work is able reduce the effect of singularity as well as instability of previous model.

From the results, both schemes discussed in chapter 4 are able to reduce the instability of AWE. From the comparison, we can conclude that AWE using ML results is in close proximity with Runge-Kutta compared to AWE-ME. However, AWE-ME scheme is 3.3 times faster than the conventional solver, namely Runge-Kutta (RK) and need 1.7 times less computational time than AWE with ML scheme. Despite this, the AWE-ML is more accurate for predicting the initial frequency as well as delay based on the close proximity with Runge-Kutta, hence emerges as the most stable and accurate technique to analyse the fast transient thermal analysis of non-Fourier heat conduction model when compared to ICAWE, partial Pade AWE, and AWE-ME.

5 CHAPTER 5: TICKONOV BASED WCAWE

Though the results obtained from AWE with ML scheme are accurate and successfully approximate the initial delay, but the method is computationally expensive compare to AWE and AWE with ME. Moreover, the correction term chosen from Z matrix; which is arbitrary chosen. In this dissertation, we have developed another moment matching based method namely Tikhonov based Well-conditioned asymptotic waveform evaluation (TWCAWE). The TWCAWE method is discussed in following section. In TWCAWE method, we are able to calculate Z matrix instead of choosing arbitrarily and also faster than AWE.

5.1 Motivation

A Tikhonov based well-conditioned AWE (TWCAWE) moment-matching process is proposed for matrix equations (like the frequency-domain FEM) that have polynomial variations in the MORE parameter. Unlike regular AWE methods, this novel TWCAWE process is well-conditioned; therefore, it is robust and does not stagnate. Furthermore, unlike the linearized Krylov subspace methods, TWCAWE does not require the neglect of higher order terms or the introduction of extra degrees of freedom; therefore, the approximation can be accurate in a wider bandwidth with just one expansion point and the memory required to store the MORE vectors does not become prohibitive for large-scale FEM problems.

5.2 TWCAWE moment matching process

Consider a model of physical phenomenon

$$K(s)x(s) = F(s) \quad (5.1)$$

where $K(s)$ is compound matrix, $F(s)$ is the compound excitation vector, $x(s)$ is key vector and $s=j2\pi f$. Consider an extension point $s_0(s_0=j2\pi f_0)$ and the Taylor series is denoted by equation (5.2).

$$\sum_{n=0}^{b_1} (s - s_0)^n K_n x(s) = \sum_{n=0}^{c_1} (s - s_0)^n F_n \quad (5.2)$$

Where, b_1 and c_1 are selected large enough so that no substantial higher order terms of K_n and/or F_n are trimmed.

The moments matching AWE subspaces for Equation (5.1) are rendering to Equation (5.3), the moments are following

$$\hat{m}_1 = K_0^{-1} F_0$$

$$\hat{m}_2 = K_0^{-1} (F_1 - K_1 \hat{m}_1)$$

$$\hat{m}_3 = K_0^{-1} (F_2 - K_2 \hat{m}_2)$$

.

.

.

$$\hat{m}_q = K_0^{-1} (F_{q-1} - \sum_{d=1}^{q-1} K_d \hat{m}_{q-d}) \quad (5.3)$$

The above moments are linearly dependent for trivial values of q as monotonous pre-multiplied by K_0^{-1} . To avoid all these difficulties mention in above chapter, moments are calculated in alternative way in TWCAWE model; which able to produce significant results for any values of q . Consider TWCAWE moment subspace are $\hat{V} = (\hat{v}_1, \hat{v}_2, \dots, \hat{v}_n)$

Table 5.1: ALGORITHM 1

1	$\hat{v}_1 = K_0^{-1} F_0$
2	$Z_{[1,1]} = \ \hat{v}_1\ $
3	$\hat{w}_1 = \hat{v} Z_{[1,1]}^{-1}$
4	for $r=2,3,\dots,n$
5	$\hat{v}_r = K_0^{-1} \left(\sum_{m=1}^{r-1} \left(F_m e_1^T J_{U_1}(r,m) - K_1 \hat{w}_{r-1} - \sum_{m=2}^{r-1} K_m \hat{w}_{r-m} J_{U_2}(r,m) e_{r-m} \right) \right)$
6	for $p=1,2,3,\dots,(r-1)$ do
7	$Z_{[p,r]} = \hat{w}_p^H \hat{v}_r$
8	$\hat{v}_n = \hat{v}_n - Z_{[p,r]} \hat{w}_p$
9	$Z_{[r,r]} = \ \hat{v}_r\ , \hat{w}_r = \hat{v}_r Z_{[r,r]}^{-1}$

Here we simplified certain scheme:

$$J_{U_w}(r,m) = \prod_{i=1}^m Z_{[ir-m+i-1, ir-m+i-1]}$$

And e_r is the r^{th} unit vector: all its entries are 0 excluding the r^{th} , which is 1.

5.3 Significance of Z matrix

Note that, no constraints have been placed on the matrix except that it is upper-triangular and non-singular. This freedom to choose can be exploited to show that TWCAWE is actually a generalization of both the AWE and Arnoldi processes. In particular, if is chosen as the identity matrix, then it is trivial to see that the TWCAWE vectors reduce to the AWE vectors. On the other hand, in (Slone, 2002), it is shown that it is possible to choose in such a way that the Arnoldi vectors for an expanded, linearized system (Cullum, Ruehli, & Zhang, 2000) can be produced from the well-conditioned vectors . The choice for that will accomplish this is very complicated and beyond the scope of this paper. Neither of these choices for is used in this work. Of course, on one hand the desire to avoid the ill-conditioned AWE vectors is clear. On the other hand, choosing in such a way that the Arnoldi vectors can be produced is not only very complicated but also not necessarily the best choice. This is because, as will be seen in the numerical examples section, TWCAWE with chosen as the modified Gram–Schmidt coefficients required to orthonormalize gives a more accurate solution than a projection via Arnoldi process on the expanded, linearized matrix described in (Cullum et al., 2000).

5.4 Breakdown of WCAWE

In present work, TWCAWE model has been used to imprecise the temperature responses in diverse boundary conditions. In some specific circumstances, the algorithm might breakdown (Ramón Quintanilla & Racke, 2006; Soproniuk, 2007; Souza Lenzi et al., 2013). Assume, the Taylor coefficient matrices are: K_0 , $K_1=K_0$, $K_2 \neq K_0$ and right hand side follow the identical pattern, the moments rendering to Equation (5.3) are

$$\hat{m}_1 = K_0^{-1} F_0$$

$$\hat{m}_2 = K_0^{-1} (F_1 - K_1 \hat{m}_1)$$

$$\hat{m}_2 = K_0^{-1} (F_0 - K_0 K_0^{-1} F_0) = 0$$

$$\hat{m}_3 = K_0^{-1} (F_2 - K_1 \hat{m}_2 - K_2 \hat{m}_1)$$

$$\hat{m}_3 = K_0^{-1} (F_2 - K_2 K_0^{-1} F_0) \neq 0$$

TWCAWE model, represented in Algorithm 1, in additional precision for this case produces the following

$$\text{i) } \hat{v}_1 = K_0^{-1} F_0, Z_{[1,1]} = \|\hat{v}_1\| \Rightarrow \hat{w}_1 = \hat{v}_1 Z_{[1,1]}^{-1}$$

$$\text{ii) } \hat{v}_2 = K_0^{-1} (F_0 e_1^T J_{U_1} (2,1) e_1 - K_1 \hat{w}_1) = \zeta$$

$$\text{iii) } Z_{[1,2]} = \hat{w}_1^H \hat{v}_2 = \zeta \Rightarrow \hat{v}_2 = \hat{v}_2 - Z_{[1,2]} \hat{w}_2 = \zeta$$

$$\text{iv) } Z_{[2,2]} = \|\hat{v}_2\| = \zeta \Rightarrow \hat{w}_2 = \hat{v}_2 Z_{[2,2]}^{-1} = \zeta / \zeta$$

where ζ is a vector with entries below machine precision. To evade the breakdown, the modified TWCAWE algorithm is shown in following Table 5.2.

Table 5.2: ALGORITHM 2

1	$\hat{v}_1 = K_0^{-1} F_0$
2	$Z_{[1,1]} = \ \hat{v}_1\ $
3	$\hat{w}_1 = \hat{v}_1 Z_{[1,1]}^{-1}$
4	for $r=2,3,\dots,n$
5	$k = 1, \hat{v}_1 = \hat{w}_1$

$$6 \quad \hat{v}_r = K_0^{-1} \left(\sum_{m=1}^{r-1} \left(F_m e_1^T J_{U_1}(r, m) - K_1 \hat{w}_{r-1} - \sum_{m=2}^{r-1} K_m \hat{w}_{r-m} J_{U_2}(r, m) e_{r-m} \right) \right)$$

$$7 \quad \text{for } p=1,2,3,\dots,(r-1) \text{ do}$$

$$8 \quad Z_{[p,r]} = \hat{w}_p^H \hat{v}_r$$

$$9 \quad \hat{v}_n = \hat{v}_n - Z_{[p,r]} \hat{w}_p$$

$$10 \quad Z_{[r,r]} = \|\hat{v}_r\|, \hat{w}_r = \hat{v}_r Z_{[r,r]}^{-1}$$

After calculating the TWCAWE moments using algorithm 2 that shown in Table 5.2, the new poles and residues can be found by using the equation (3.15)- (3.20). The final transient response can be found by using the Equation 3.21. The working flow is same as the flowchart shown in Figure 3.4.

5.5 Numerical Example

In the present study, the Fourier and non-Fourier heat transfer is investigated by considering two dimensional rectangular models. The heat conduction model with dual phase delay has been explained by using finite element analysis. For heating flux, three distinctive temporal profiles, such as

- (i) Instantaneous heat impulse
- (ii) Constant heat imposed
- (iii) Periodic type

Above three temperature profiles are preferred because those boundary conditions are widely used in engineering problems. In the case of Fourier heat conduction, we have

used instantaneous heat impulse only. But in the case of Non-Fourier heat conduction, we have used above three boundaries condition. Diverse boundary conditions are executed at the left edge of the slab. The three type of boundary condition are shown in below Figure (5.1)-(5.3)

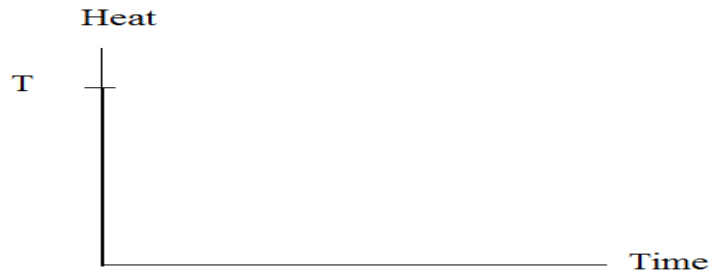


Figure 5.1: Instantaneous heat impulse

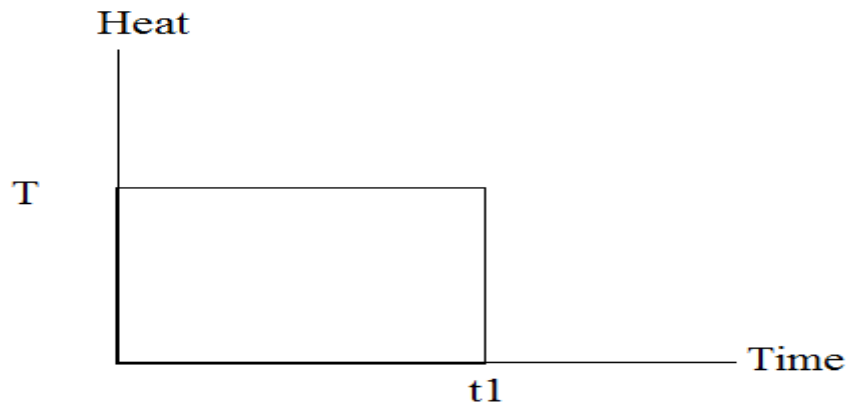


Figure 5.2: Constant heat imposed

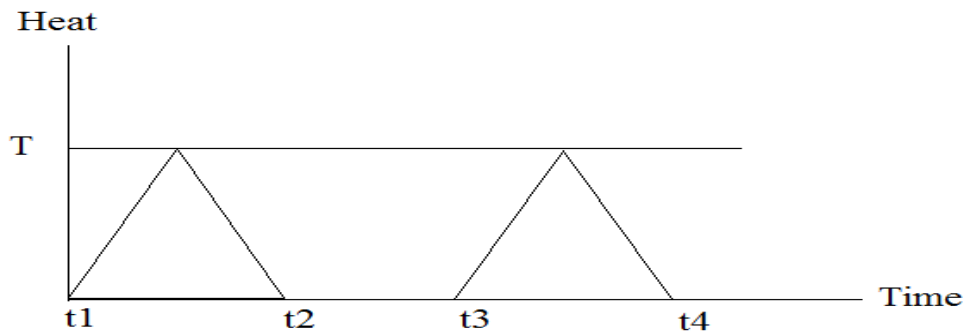


Figure 5.3: Periodic heat imposed

5.5.1 Observation of Fourier heat conduction

The Figure 5.4 shows the rectangular slab with instantaneous temperature imposed left edge of the slab. Figure 5.5 and Figure 5.6 exemplify the Fourier temperature responses respecting normalized time and normalized distance correspondingly with instant heat imposed left edge of the boundary. The results demonstrate that, the thermal influence is sensed instantaneously throughout the system if the surface of a material is heated. This leads to simultaneous development of heat flux and temperature gradient. Classical Fourier law assumes that instantaneous thermal equilibrium between electron and phonons. Figure 5.5 and Figure 5.6 also spectacles that, when instantaneous heat executed left edge of the boundary the same thermal effect felt right edge of the slab instantly.

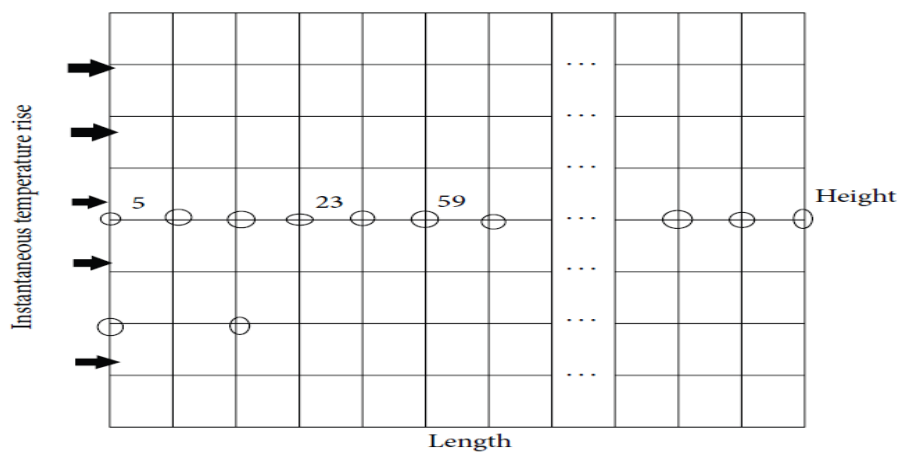


Figure 5.4: Two-dimensional slab subjected to instantaneous temperature rise on left edge.

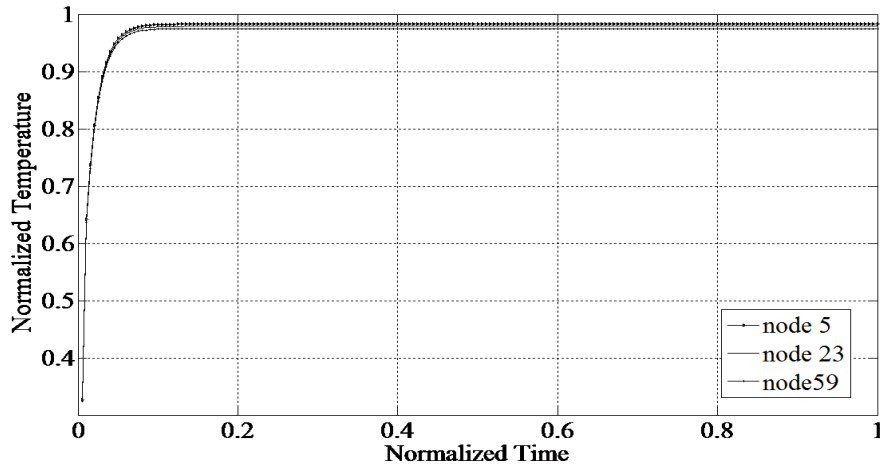


Figure 5.5: Normalized temperature responses for Fourier heat conduction

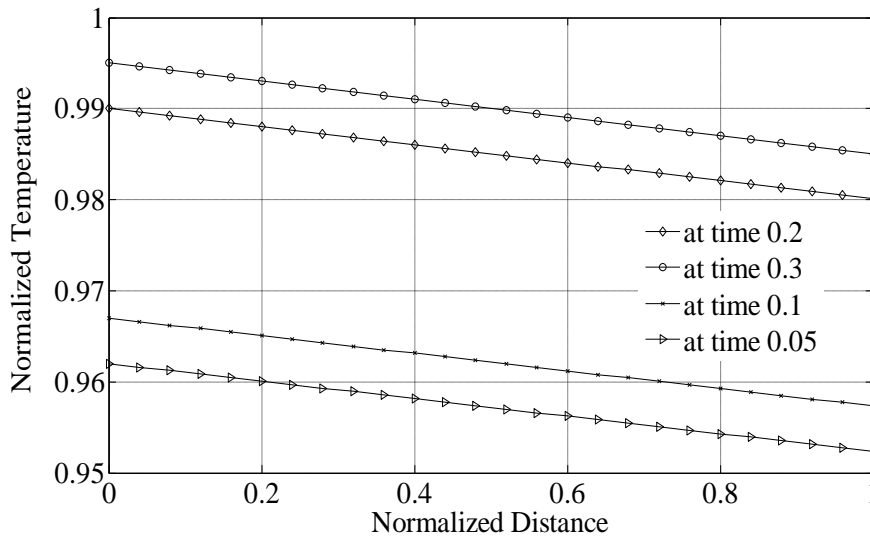


Figure 5.6: Fourier temperature responses along the centre of the slab for different time

5.5.2 TWCAWE with different boundary condition

In the present work, three distinct boundary conditions are investigated for non-Fourier heat conduction. The phase delays are varied to spectacle the comparative significance of the wave term and the phonon-electron collaboration. In this work, to authenticate the TWCAWE results, we compared the results with R-K outcomes. Figures 5.7 to 5.12 exemplify the temperature responses for non-Fourier heat conduction by using three typical temperature profiles. In these figures, we have compared the results of three different numerical techniques, such as Runge-Kutta (R-K), AWE and TWCAWE to

prove the accuracy. In these comparisons, we have used similar experimental settings of total length and width of the slab, total number of nodes, thermal conductivity and imposed temperature for the above mentioned methods. In this study, the fourth order R-K method has been taken as an exact analytical technique as a benchmark, since the results obtained from this technique is accurate, but computationally expensive.

Figure 5.7(A) and Figure 5.7(B) displays the temperature spreading of sudden heat executed on the left edge of the slab, also signifies the comparison of TWCAWE, R-K and AWE methods for diverse values of Z_b at node 5 and node 59, respectively. It can be observed that, at node 5, initial fluctuation has been reduced, which helps to approximate the temperature behavior of other node accurately (e.g., node 59), as shown in Figure 5.7.

This evaluation spectacle that, TWCAWE results absolutely match with the R-K outcome for $Z_b=0.5$ and 0.05 , but AWE results show inconsistency. For the instance of $Z_b=0.0001$, TWCAWE congregates to similar steady state as R-K. Before uniting to the steady-state, R-K results display convergence with TWCAWE, but AWE is incompetent to forecast the accurate temperature response as TWCAWE and R-K due to instability of AWE. It can be also observed from Figure 5.7 that, for TWCAWE method, the temperature behaviours are converged after normalized time of 0.25 and 0.31 in case of $Z_b=0.05$ and $Z_b=0.0001$, respectively at node 5. In case of node 59, the temperature behaviours are converged after normalized time of 0.5 and 0.9 for $Z_b=0.05$ and $Z_b=0.0001$, respectively; because the node 59 is far from the boundary where temperature imposed, as shown in Figure 5.4.

Figure 5.8(A), 5.8(B), 5.8(C) and 5.8(D) displays the non-Fourier temperature circulation respecting distance along the centre of the slab at time 0.005, 0.05, 0.1 and 0.5, correspondingly for TWCAWE. This temperature distribution with instant heat

executed at boundary conditions for $Z_b=0.5, 0.05$ and 0.0001 . Immediate heat pulse is imposed on the left edge of the slab and the heat is drifting towards the other edge of the slab. Figure 5.8 also shows the evaluation of TWCAWE, R-K and AWE outcomes. The evaluation shows the TWCAWE results precisely adjacent to R-K solution, but AWE shows inconsistency.

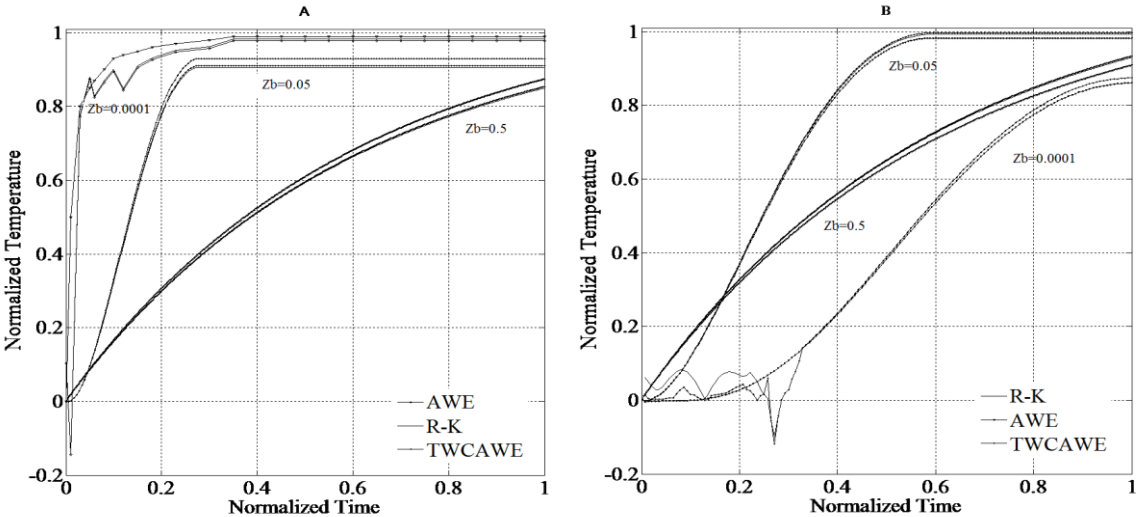


Figure 5.7: Normalized temperature responses along the Centre of the slab for $Z_b=0.5, 0.05$ and for $Z_b=0.0001$ with instantaneous heat imposed, A) at node 5, B) at node 59

Figure 5.9 and Figure 5.10 points to the non-Fourier temperature responses for intervallic heat imposed at the left edge of the slab. Figure 5.9 (A) and Figure 5.9 (B) signify the temperature dissemination with veneration to time for $Z_b=0.5, 0.05$ and 0.0001 at node 5 and node 59 correspondingly. Figure 5.10 and Figure 5.11 spectacles the temperature responses with persistent heat enacted left edge of the rectangular slab

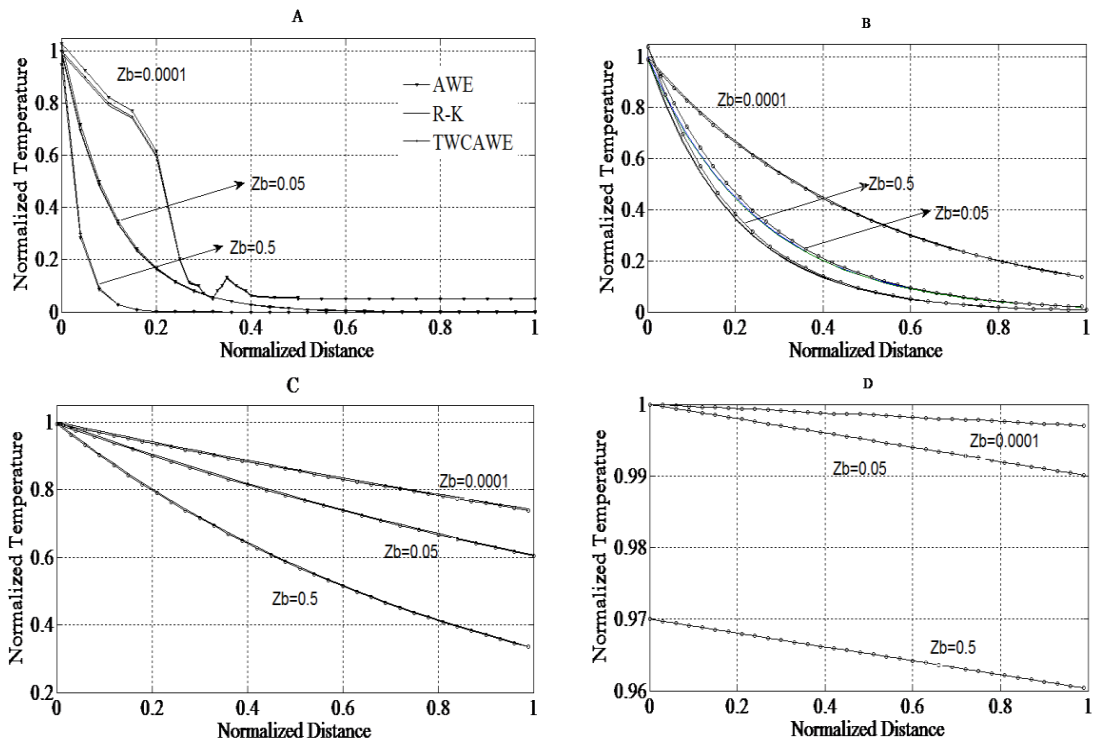


Figure 5.8: Normalized temperature distribution along centre of the slab for $Z_b=0.5, 0.05$ and $Z_b=0.0001$ with instantaneous heat imposed (A) at time 0.005 (B) at time 0.05 (C) at time 0.1 (D) at time 0.5

These figures also epitomize the evaluation of TWCAWE, RK and AWE. These figures spectacles that, TWCAWE results utterly matched with RK outcomes on behalf of $Z_b=0.5$ and 0.05 , but in this instance AWE results show divergence. In the case of $Z_b=0.0001$, TWCAWE converges to similar steady state as RK. Before converging to the steady-state, AWE outcomes are inept to envisage the accurate temperature response as TWCAWE. By investigates three diversities of boundary condition results, it is perceived that, the heat conveyance promptness is penetrating to the way in which the boundary condition are quantified and TWCAWE technique efficaciously imprecise delay precisely.

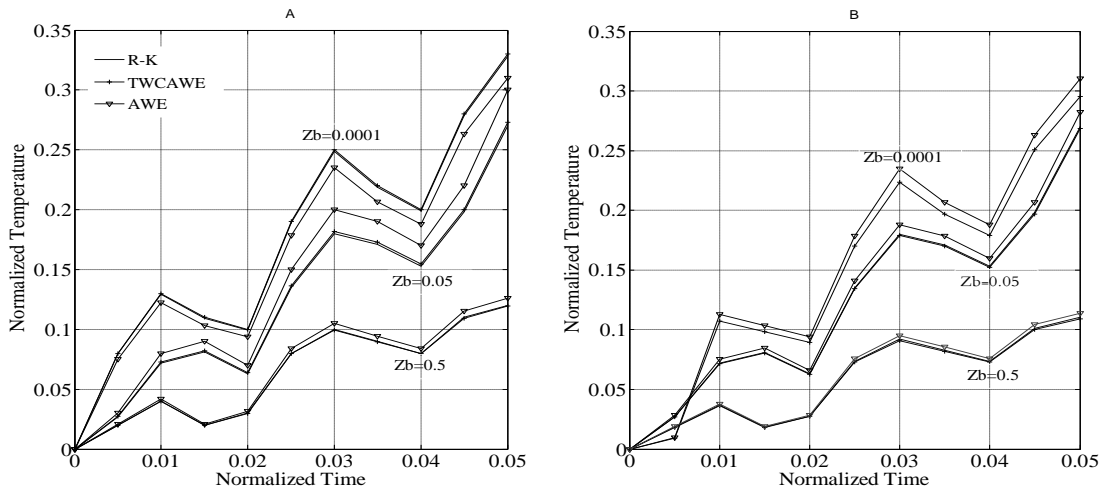


Figure 5.9: Normalized temperature response along centre of the slab for $Z_b=0.5$, 0.05 and $Z_b=0.0001$ with periodic heat executed, A) at node 5, B) at node 59

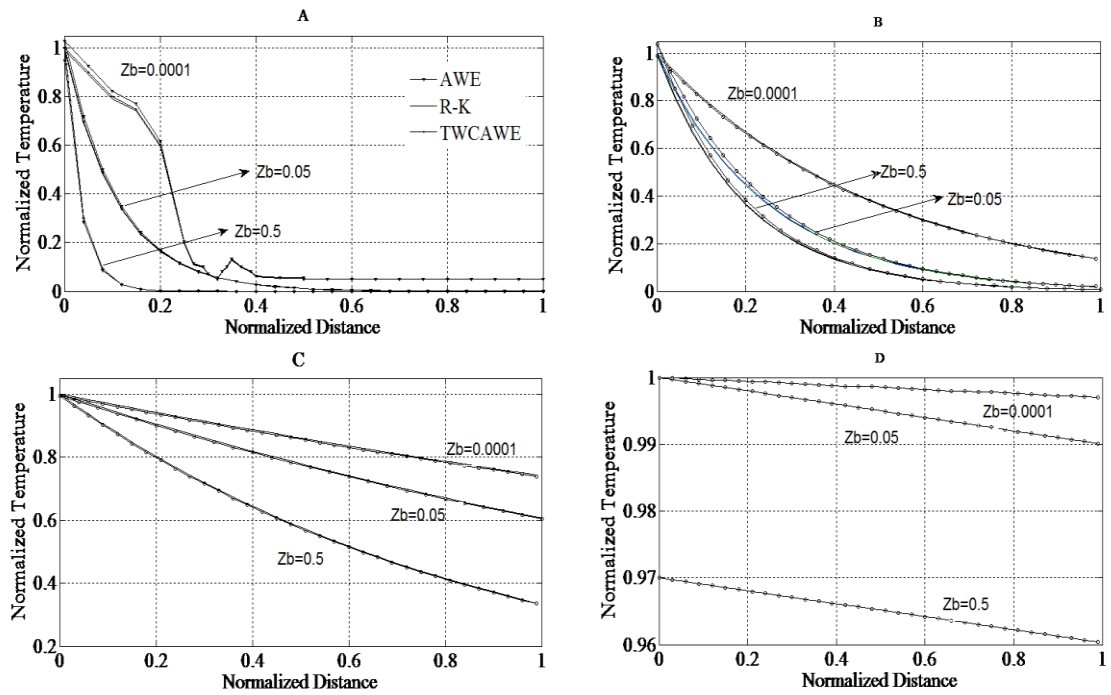


Figure 5.10: Normalized temperature distribution along the centre of the slab for three values of Z_b with periodic heat levied, A) at time 0.005, B) at time 0.05, C) at time 0.1, D) at time 0.5

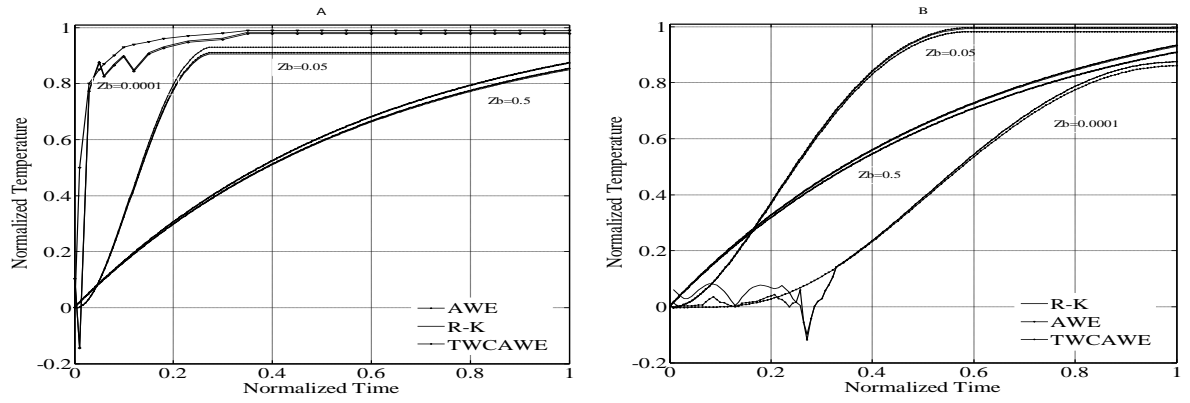


Figure 5.11: Normalized Temperature response along for three values of Z_b with constant heat imposed, A) at node 5, B) at node 59

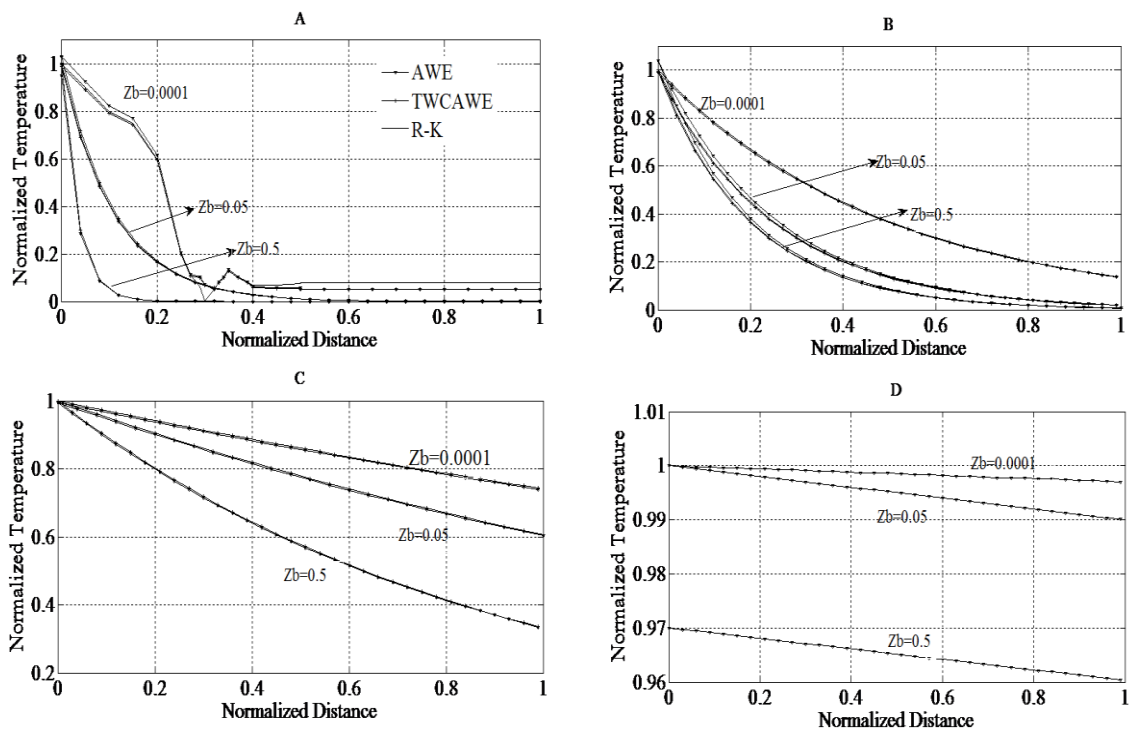


Figure 5.12: Normalized temperature dissemination along the centre of the slab for three values of Z_b with constant heat imposed, A) at time 0.005, B) at time 0.05, C) at time 0.1, D) at time 0.5

In the current work, we propose a TWCAWE method to investigate the Fourier and non-Fourier heat conduction in different boundary conditions, which implanted with Tikhonov regularization technique to enrich the immovability. In this proposed TWCAWE model, no need to renovate non-Fourier heat conduction equation into linear equation. In the current study, we are capable to find out the Z matrix mathematically

instead of choosing randomly, which assists to find out the correction term efficiently. The results attained from TWCAWE method precisely matched with Runge-Kutta (R-K) results and also competent to remove all instabilities of AWE. Additionally, the method proposed in the current work is 1.2 times faster compared to AWE.

6 CHAPTER 6: SUMMARY AND CONCLUSION

6.1 Summary of the finding and conclusion drawn

In the present work, the heat conduction based on DPL has solved using FEM. The phase lag responsible for finite relaxation time, that is varied to verify the capability of our proposed model for predicting the temperature responses in two dimensional model. Several analytical method have analysed, one of them is iteration based namely Runge-Kutta. The results obtained from RK are accurate but computationally expensive. In this dissertation, RK results are taken as benchmark to compare with the results obtained from other moment matching based method to justify their accuracy. To reduce the computational time, moment matching based method namely AWE has introduced. AWE method is 3 times faster than RK method. But unfortunately, AWE moments matching is intrinsically ill-conditioned.

In the present work, we have introduced two Tikhonov based well-conditioned scheme namely AWE with ML and AWE with ME. In comparison, the temperature responses obtained from AWE with ML are closer to RK than AWE with ME. Unfortunately, AWE with ML method is not faster as AWE with ME and ICAWE. Furthermore, Z matrix has chosen arbitrarily in AWE with ML method. Then we have developed another moment matching based method namely TWCAWE which is able to analyse the non-Fourier heat transfer in different boundary condition.

Table 6.1: Simulation time required by different method.

Method Name	Time (s)	Ratio with respect to RK
Runge-Kutta	16	1
AWE with ML	8.2	1.95
AWE with ME	4.8	3.33
ICAWE	4.8	3.33
ICAWE with partial Pade	4.8	3.33
TWCAWE	4	4

Table 6.1 shows the computational time required by different method have discussed in the present work. In these comparisons, we have used similar experimental settings of total length and width of the slab, total number of nodes, thermal conductivity and imposed temperature for the above mentioned methods. From the table, AWE using ML found to be almost two times faster than Runge-Kutta. The orthonormalization and maximum likelihood approximation process in AWE-ML poses computational load that makes it slower compared to ICAWE or partial Pade AWE. As AWE using ME does not require orthonormalization and maximum likelihood approximation, it performs as fast as ICAWE or AWE using partial Pade despite some sacrifice in temperature response quality in comparison to AWE- ML. But AWE-ME showed more stable and hence accurate results compared to either ICAWE or AWE using partial Pade. TWCAWE method is 4 times faster than RK and 1.2 times faster than AWE.

This dissertation recommends the TWCAWE method to illustrate the non-Fourier heat conduction in diverse boundary conditions; there is no need to linearize the matrix equation and also no need to announce additional degree of freedom. Lastly, during moment calculation, we are competent to evaluate Z matrix mathematically for this

problem. The numerical comparison presented in this work demonstrates that, TWCAWE method is precise and well-conditioned since this technique is able to approximate the delay and initial high frequencies precisely. The numerical specimens also indicate that, the results are very subtle in the way in which the boundary conditions are quantified. Additionally, it is found that, TWCAWE is 1.2 times faster than the ICAWE, but 4 times faster than the R-K. Moreover, the results are considerably superior than the ICAWE.

7 REFERENCES

- Gwennap, Linley. (1998). Alpha 21364 to ease memory bottleneck. *Microprocessor Report*, 12(14), 12-15.
- Bai, Cheolho, & Lavine, Adrienne S. (1991). *Hyperbolic heat conduction in a superconducting film*. Paper presented at the ASME/JSME Thermal Engineering Joint Conference, Reno, NV.
- Banerjee, Kaustav, Mehrotra, Amit, Sangiovanni-Vincentelli, Alberto, & Hu, Chenming. (1999). *On thermal effects in deep sub-micron VLSI interconnects*. Paper presented at the Proceedings of the 36th annual ACM/IEEE Design Automation Conference.
- Baumeister, KJ, & Hamill, TD. (1969). Hyperbolic heat-conduction equation—a solution for the semi-infinite body problem. *Journal of heat transfer*, 91(4), 543-548.
- Baumeister, KJ, & Hamill, TD. (1971). Discussion:“Hyperbolic Heat-Conduction Equation—A Solution for the Semi-Infinite Body Problem”(Baumeister, KJ, and Hamill, TD, 1969, ASME J. Heat Transfer, 91, pp. 543–548). *Journal of Heat Transfer*, 93(1), 126-127.
- Bloembergen, N, Kurz, H, Liu, JM, & Yen, R. (1981). *Fundamentals of energy transfer during picosecond irradiation of silicon*. Paper presented at the MRS Proceedings.
- Brown, JB, Chung, DY, & Matthews, PW. (1966). Heat pulses at low temperatures. *Physics Letters*, 21(3), 241-243.
- Burke, GJ, Miller, EK, Chakrabarti, S, & Demarest, K. (1989). Using model-based parameter estimation to increase the efficiency of computing electromagnetic transfer functions. *Magnetics, IEEE Transactions on*, 25(4), 2807-2809.
- Chandrasekharaiah, DS. (1998). Hyperbolic thermoelasticity: a review of recent literature. *Applied Mechanics Reviews*, 51(12), 705-729.
- Cheah, TS, Seetharamu, KN, Ghulam, AQ, Zainal, ZA, & Sundararajan, T. (2000). *Numerical modelling of microscale heat conduction effects in electronic package for different thermal boundary conditions*. Paper presented at the Electronics Packaging Technology Conference, 2000.(EPTC 2000). Proceedings of 3rd.
- Chester, Marvin. (1963). Second sound in solids. *Physical Review*, 131, 2013-2015.
- Choudhuri, SK Roy. (2007). On a thermoelastic three-phase-lag model. *Journal of Thermal Stresses*, 30(3), 231-238.
- Cullum, Jane, Ruehli, Albert, & Zhang, Tong. (2000). A method for reduced-order modeling and simulation of large interconnect circuits and its application to PEEC models with retardation. *Circuits and Systems II: Analog and Digital Signal Processing, IEEE Transactions on*, 47(4), 261-273.
- Gibbons, James Franklin, Sigmon, TW, & Hess, Laverne Derryl. (1981). Laser and Electron-beam Solid Interactions and Materials Processing: Proceedings of the

Materials Research Society Annual Meeting, November 1980, Copley Plaza Hotel, Boston, Massachusetts, USA (Vol. 1): North Holland.

- Govinder, KS, & Govender, M. (2001). Causal solutions for radiating stellar collapse. *Physics Letters A*, 283(1), 71-79.
- Green, AE, & Naghdi, PM. (1992). On undamped heat waves in an elastic solid. *Journal of Thermal Stresses*, 15(2), 253-264.
- Gwennap, Linley. (1998). Alpha 21364 to ease memory bottleneck. *Microprocessor Report*, 12(14), 12-15.
- Hetnarski, RB, & Ignaczak, J. (2000). Nonclassical dynamical thermoelasticity. *International Journal of Solids and Structures*, 37(1), 215-224.
- Hetnarski, Richard B, & Ignaczak, Jozef. (1999). Generalized thermoelasticity. *Journal of Thermal Stresses*, 22(4-5), 451-476.
- Horowitz, J Rubinstein P Penfield MA. (1983). Signal delay in RC tree networks. *IEEE transactions on computer-aided design*, 2(3).
- Lanczos, Cornelius. (1950). An iteration method for the solution of the eigenvalue problem of linear differential and integral operators: United States Governm. Press Office.
- Liu, Da-Guang, Phanilatha, V, Zhang, Qi-Jun, & Nakhla, Michel S. (1995). Asymptotic thermal analysis of electronic packages and printed-circuit boards. *Components, Packaging, and Manufacturing Technology, Part A, IEEE Transactions on*, 18(4), 781-787.
- Liu, Pu, Li, Hang, Jin, Lingling, Wu, Wei, Tan, SX, & Yang, Jun. (2006). Fast thermal simulation for runtime temperature tracking and management. *Computer-Aided Design of Integrated Circuits and Systems, IEEE Transactions on*, 25(12), 2882-2893.
- Loh, JS, Azid, IA, Seetharamu, Kankanally N, & Quadir, Ghulam Abdul. (2007). Fast transient thermal analysis of Fourier and non-Fourier heat conduction. *International journal of heat and mass transfer*, 50(21), 4400-4408.
- Marín, E. (2013). Thermal Wave Physics and Related Photothermal Techniques: Basic Principles and Recent Developments.
- Marín, E, Marín-Antuña, J, & Díaz-Arencibia, P. (2002). On the wave treatment of the conduction of heat in photothermal experiments with solids. *European journal of physics*, 23(5), 523.
- Marín, E, Marin, J, & Hechavarría, R. (2005). *Hyperbolic heat diffusion in photothermal experiments with solids*. Paper presented at the Journal de Physique IV (Proceedings).
- Maxwell, J Clerk. (1867). On the dynamical theory of gases. *Philosophical Transactions of the Royal Society of London*, 49-88.

- McCormick, Steven Paul. (1989). Modeling and simulation of VLSI interconnections with moments. Citeseer.
- Mishra, Subhash C, & Roy, Hillol K. (2007). Solving transient conduction and radiation heat transfer problems using the lattice Boltzmann method and the finite volume method. *Journal of Computational Physics*, 223(1), 89-107.
- Neumaier, Arnold. (1998). Solving ill-conditioned and singular linear systems: A tutorial on regularization. *Siam Review*, 40(3), 636-666.
- Ooi, CK, Seetharamu, Kankanhally N, Alauddin, ZAZ, Quadir, GA, Sim, KS, & Goh, Teck Joo. (2003a). *Fast transient solutions for heat transfer [FEM]*. Paper presented at the TENCON 2003. Conference on Convergent Technologies for the Asia-Pacific Region.
- Ooi, CK, Seetharamu, KN, Alauddin, ZAZ, Quadir, GA, Sim, KS, & Goh, TJ. (2003b). *Fast transient solutions for heat transfer [FEM]*. Paper presented at the TENCON 2003. Conference on Convergent Technologies for the Asia-Pacific Region.
- Ozisik, MN, & Tzou, DY. (1994). On the wave theory in heat conduction. *Journal of Heat Transfer*, 116(3), 526-535.
- Pillage, Lawrence T, Huang, Xiaoli, & Rohrer, Ronald A. (1989). *AWESim: asymptotic waveform evaluation for timing analysis*. Paper presented at the Design Automation, 1989. 26th Conference on.
- Pillage, Lawrence T, & Rohrer, Ronald A. (1990). Asymptotic waveform evaluation for timing analysis. *Computer-Aided Design of Integrated Circuits and Systems, IEEE Transactions on*, 9(4), 352-366.
- Prakash, G Siva, Reddy, S Sreekanth, Das, Sarit K, Sundararajan, T, & Seetharamu, KN. (2000). Numerical modelling of microscale effects in conduction for different thermal boundary conditions. *Numerical Heat Transfer: Part A: Applications*, 38(5), 513-532.
- Quintanilla, R. (2002). Exponential stability in the dual-phase-lag heat conduction theory. *Journal of Non-Equilibrium Thermodynamics*, 27(3), 217-227.
- Quintanilla, Ramón, & Racke, Reinhard. (2006). A note on stability in dual-phase-lag heat conduction. *International Journal of Heat and Mass Transfer*, 49(7), 1209-1213.
- Quintanilla, Ramón, & Racke, Reinhard. (2007). Qualitative aspects in dual-phase-lag heat conduction. *Proceedings of the Royal Society A: Mathematical, Physical and Engineering Science*, 463(2079), 659-674.
- Rzepka, Sven, Banerjee, Kaustav, Meusel, Ekkehard, & Hu, Chenming. (1998). Characterization of self-heating in advanced VLSI interconnect lines based on thermal finite element simulation. *IEEE Transactions on Components, Packaging, and Manufacturing Technology*, 21(3), 406-411.

- Slone, Rodney Daryl. (2002). Fast frequency sweep model order reduction of polynomial matrix equations resulting from finite element discretizations. The Ohio State University.
- Slone, Rodney Daryl, Lee, Robert, & Lee, Jin-Fa. (2003). Well-conditioned asymptotic waveform evaluation for finite elements. *Antennas and Propagation, IEEE Transactions on*, 51(9), 2442-2447.
- Soproniuk, Yevgeny. (2007). The Practical Stability of the Linear Systems with the Phase Space Variable Measurability. *Advances in electrical and computer engineering*, 7(1), 50-53.
- Souza Lenzi, Marcos, Lefteriu, Sanda, Beriot, Hadrien, & Desmet, Wim. (2013). A fast frequency sweep approach using Padé approximations for solving Helmholtz finite element models. *Journal of Sound and Vibration*, 332(8), 1897-1917.
- Suhir, E, & Lee, Yung-Cheng. (1988). Thermal, mechanical, and environmental durability design methodologies. *Electronic Materials Handbook*, 1, 47-75.
- Sun, Yuzhi, & Wichman, Indrek S. (2004). On transient heat conduction in a one-dimensional composite slab. *International Journal of Heat and Mass Transfer*, 47(6), 1555-1559.
- Tang, DW, & Araki, N. (1996). Non-Fourier heat conduction in a finite medium under periodic surface thermal disturbance. *International journal of heat and mass transfer*, 39(8), 1585-1590.
- Tang, DW, & Araki, N. (2000). Non-fourier heat conduction behavior in finite mediums under pulse surface heating. *Materials Science and Engineering: A*, 292(2), 173-178.
- Tang, Tak K, & Nakhla, Michel S. (1992). Analysis of high-speed VLSI interconnects using the asymptotic waveform evaluation technique. *Computer-Aided Design of Integrated Circuits and Systems, IEEE Transactions on*, 11(3), 341-352.
- Vadasz, Johnathan J, Govender, Saneshan, & Vadasz, Peter. (2005). Heat transfer enhancement in nano-fluids suspensions: Possible mechanisms and explanations. *International Journal of Heat and Mass Transfer*, 48(13), 2673-2683.
- Vernotte, Pierre. (1958). La véritable équation de la chaleur. *Comptes rendus hebdomadaires des séances de l'academie des sciences*, 247(23), 2103-2105.
- Wang, Liqiu, & Xu, Mingtian. (2002). Well-posedness of dual-phase-lagging heat conduction equation: higher dimensions. *International journal of heat and mass transfer*, 45(5), 1165-1171.
- Wang, Liqiu, Xu, Mingtian, & Zhou, Xuesheng. (2001). Well-posedness and solution structure of dual-phase-lagging heat conduction. *International journal of heat and mass transfer*, 44(9), 1659-1669.
- Wang, Xiang-Qi, & Mujumdar, Arun S. (2007). Heat transfer characteristics of nanofluids: a review. *International journal of thermal sciences*, 46(1), 1-19.

Yu Tzou, Da. (1991). The resonance phenomenon in thermal waves. *International journal of engineering science*, 29(9), 1167-1177.

Zienkiewicz, Olgierd Cecil, & Taylor, Robert Leroy. (2000). *The finite element method: Solid mechanics* (Vol. 2): Butterworth-heinemann.

PUBLICATIONS

Journal papers

1. **Sohel Rana**, Kanesan Jeevan, R. Harikrishnan and Ahmed Wasif Reza, Fast Transient Thermal Analysis of Non-Fourier Heat Conduction Using Tikhonov based Well-Conditioned Asymptotic Waveform Evaluation (**ISI cited Journal, Q1**)
2. **Sohel Rana**, Kanesan Jeevan, R. Harikrishnan and Ahmed Wasif Reza, Tikhonov based well-condition asymptotic waveform evaluation for dual-phase –lag heat conduction (**ISI cited Journal, Q2**)

Conference Paper

3. **Sohel Rana**, Kanesan Jeevan, R. Harikrishnan and Ahmed Wasif Reza, A Well-Condition Asymptotic Waveform Evaluation Method for Heat Conduction Problems (1st International Materials, Industrial, and Manufacturing Conference (MIMEC 2013))
4. **Sohel Rana**, Kanesan Jeevan, R. Harikrishnan and Ahmed Wasif Reza, Analysis of Fourier and Non-Fourier heat conduction using Tikhonov based Well-conditioned Asymptotic Waveform Evaluation Technique (3rd International Conference on Computer Engineering & Mathematical Sciences (ICCEMS 2014))